

Mechanical performance and autogenous and drying shrinkage of MgO-based recycled aggregate high-performance concrete

Víctor Revilla-Cuesta^{a,e}, Luís Evangelista^{b,e}, Jorge de Brito^{c,e}, Marta Skaf^d,
Vanessa Ortega-López^{a,*}

^a Department of Civil Engineering, Escuela Politécnica Superior, University of Burgos, c/Villadiego s/n, Burgos 09001, Spain

^b Department of Civil Engineering, Instituto Superior de Engenharia de Lisboa – IPL, R. Conselheiro Emídio Navarro 1, Lisbon 1959-007, Portugal

^c Department of Civil Engineering, Architecture and Georesources, Instituto Superior Técnico, University of Lisbon, Av. Rovisco Pais 1, Lisbon 1049-001, Portugal

^d Department of Construction, Escuela Politécnica Superior, University of Burgos, c/Villadiego s/n, Burgos 09001, Spain

^e CERIS-ICIST, Instituto Superior Técnico, University of Lisbon, Av. Rovisco Pais 1, Lisbon 1049-001, Portugal

ARTICLE INFO

Keywords:

High-performance concrete
Recycled aggregates
Recycled aggregate's maturity
Magnesium oxide
Autogenous shrinkage
Drying shrinkage

ABSTRACT

The high strength and durability of high-performance concrete (HPC) may be significantly reduced by shrinkage cracking. The use of reactive magnesium oxide (MgO) can reduce shrinkage of cement-based materials due to its expansive properties. This study intends to analyse the validity of MgO as shrinkage-reducing agent in recycled aggregate HPC. To do so, ten HPC mixes with 0%, 25%, and 100% of both early-age (7-days air curing) and matured (6-month air curing) RA were produced. In half of the mixes, 10% ordinary Portland cement was replaced with MgO. The use of MgO slightly worsened the mechanical behaviour of HPC, especially when combined with large amounts of RA. On the other hand, the expansion of MgO fully offset the autogenous shrinkage of HPC and reduced total shrinkage by around 20–40%. Water storage of RA, and its deferred release over time, produced a more efficient hydration of MgO, which in turn led to a further reduction of autogenous shrinkage. However, the increase of drying shrinkage caused by RA was greater than this decrease of autogenous shrinkage due to MgO, so the higher the RA content of HPC the lower the total shrinkage reduction when adding MgO. Thus, the decrease of total shrinkage caused by MgO was compensated by the shrinkage increase because of RA when adding amounts above 35% early-age RA and 42% matured RA. Therefore, despite the suitability of MgO as shrinkage-reducing agent in recycled aggregate HPC, its effectiveness was reduced with increasing amounts of RA.

1. Introduction

Shrinkage is defined as the volumetric contraction of concrete, especially at early ages, without applying any external force [1]. This property is of great importance for the durability performance of this material, due to the cracking that it may cause [2]. The appearance of cracks favours the attack of external agents that deteriorate concrete and corrode the reinforcements, thus reducing its service life [3–5]. Therefore, shrinkage must be accurately evaluated, which is not simple, as it is a complex phenomenon caused by several factors, which are listed below.

Plastic shrinkage of concrete occurs during its transition from fresh to hardened state, due to the loss of water during this process [6]. This

shrinkage stops when a stable skeleton is formed inside concrete, *i.e.* approximately 24 h after its manufacture [7]. This moment is known as “time zero” [8]. After this, both autogenous shrinkage, which is caused by the absorption of capillary water by cement during its delayed hydration, and drying shrinkage, caused by the evaporation of the water, follow [9]. The measurement of autogenous shrinkage can be performed by isolating the concrete specimen from the environment, preventing its contact with air, so that water evaporation is blocked [10]. If the concrete specimen is left in contact with the environment, total shrinkage, which is the sum of autogenous and drying shrinkage, can be measured [11].

This study is part of a larger research that addresses the effect of different components that modify the shrinkage behaviour of high-

* Corresponding author.

E-mail addresses: vrevilla@ubu.es, vortega@ubu.es (V. Revilla-Cuesta), luis.evangelista@isel.pt (L. Evangelista), jb@civil.ist.utl.pt (J. de Brito), mksaf@ubu.es (M. Skaf), vortega@ubu.es (V. Ortega-López).

<https://doi.org/10.1016/j.conbuildmat.2021.125726>

Received 15 June 2021; Received in revised form 10 November 2021; Accepted 14 November 2021

Available online 20 November 2021

0950-0618/© 2021 The Authors.

Published by Elsevier Ltd.

This is an open access article under the CC BY-NC-ND license

(<http://creativecommons.org/licenses/by-nc-nd/4.0/>).

performance concrete (HPC) [12]. This type of concrete has a higher than usual cement content, which leads to a dense microstructure, and provides high strength and durability [13]. However, this also leads to a very high hydration heat, which increases shrinkage cracking [14]. For that reason, any modification of the composition of HPC must be carried out considering how the use of each raw material will affect this property [15], as the effect of each mix change on the shrinkage of HPC is relevant.

In recent years, the effect of replacing natural aggregates (NA) with recycled aggregates (RA) in HPC has been studied in detail [16,17]. It has been found that the simultaneous addition of coarse and fine RA reduced the mechanical properties of HPC [18], although to a lesser extent than in conventional vibrated concrete because of its denser microstructure [19]. Thus, while reductions of 40% of the mechanical properties of conventional concrete can be obtained when adding 100% coarse RA [20], those reductions for HPC have been found to be from 15% to 20%, for full replacement of coarse NA with RA [14]. On the other hand, it has also been proved that the higher water absorption and lower stiffness of RA, compared to NA, also modifies the shrinkage behaviour of HPC [21]. Maintaining the workability of HPC constant, the addition of RA reduces autogenous shrinkage by releasing water at a later stage, which replaces the capillary water absorbed by the delayed hydration of cement, in a process called internal curing [22]. However, drying shrinkage increases due to the greater amount of water released by the aggregates that subsequently evaporates [23]. In short, due to all the aspects described, the total shrinkage of HPC increases when adding RA [24].

RA can be produced at different times between casting and crushing of the parent concrete (PC), *i.e.*, RA can have different maturities. This notably affects the mechanical and shrinkage behaviour of HPC. On the one hand, the strength and stiffness of early-age RA increase over time [25], which leads to a worsening of all mechanical properties compared to those of the mixes manufactured with matured RA [26]. On the other hand, if early-age RA (e.g. after 7 days of curing) are used, both RA and the cementitious matrix will shrink when HPC is already produced [10]. Therefore, the use of early-age RA will increase all types of shrinkage. Finally, a linear relationship between RA content and shrinkage of the HPC mixes can usually be detected regardless of RA's maturity [21].

Magnesium oxide (MgO) is a chemical compound obtained from minerals such as magnesite, and whose hydration leads to the formation of magnesium hydroxide, also known as brucite ($\text{Mg}(\text{OH})_2$), as shown in Eq. (1) [27]. This reaction, which can occur at room temperature, is expansive, as the volume of brucite is greater than that of the MgO before hydration [28], and provides MgO with a suitable mechanical strength [29]. All these aspects mean that MgO can be useful as a shrinkage-reducing agent in cement-based materials [30], in the same way as other alternative binders [31]. Nevertheless, the MgO content in ordinary Portland cement has traditionally been limited to 5% (EN 197-1 [32]). This limitation is justified by the fact that the high temperatures (around 1500 °C) reached during the clinkerization process produce MgO with a late reactivity (hard-burned MgO). This, in turn, could cause it to expand when concrete already has a stable and compact microstructure, and may therefore cause micro-cracks and a great worsening of the mechanical behaviour of concrete [33]. However, if the minerals from which MgO is obtained are subjected to relatively low temperatures, between 700 and 1000 °C, it is possible to obtain light-burned or reactive MgO [34], which is able to expand at early ages (a few hours after mixing with water) due to its greater reactivity [29]. Therefore, if reactive MgO is added to concrete, its expansion occurs when the cementitious matrix of concrete has lower stiffness [35]. Thus, this reaction causes a reduced internal damage to concrete and, therefore, it is possible to take advantage of the expansive properties of this product [36].



So far, the use of reactive MgO has been validated exclusively regarding the production of cement pastes and mortars. Recent studies have shown that reactive MgO as cement replacement in relatively high quantities (10–20%) can be successfully used to produce mortars with improved shrinkage behaviour [37], reducing both autogenous [38] and total shrinkage [39]. The decrease in total shrinkage obtained for a MgO content of only 10% was between 18 and 49%, depending on its fineness [40]. On the other hand, the use of reactive MgO has allowed producing more sustainable mortars since CO₂ emissions during its manufacture represent 30% of those produced during the manufacture of cement clinker [41]. Furthermore, its effect is not changed when combined with RA, so a MgO content of 10% has also allowed reducing around 30–60% the increase in total shrinkage caused by the addition of 100% fine RA [40]. However, it has also been concluded that the use of reactive MgO in mortars generally produces a slight loss of strength [42], around 10–20% for 10% MgO as cement replacement [43].

This study intends to extend the possible field of application of reactive MgO to HPC. Thus, this article evaluates in detail the effect of a relatively high content (10%) of reactive MgO on the mechanical and shrinkage behaviour (autogenous, drying, and total shrinkage) of HPC, an aspect not studied until now and which constitutes the main novelty of this article. Moreover, this study also evaluates other novel aspects such as the interaction between reactive MgO and coarse and fine RA of different maturities, with the aim of also assessing the suitability of this product for the manufacturing of recycled aggregate HPC. To analyse all these aspects, ten HPC mixes were manufactured in this study, five of them with 10% reactive MgO as cement replacement. In addition, RA contents of 0%, 25% and 100% (simultaneous replacement of the coarse and fine fractions of NA) and two completely different maturities of RA (time between manufacturing of the parent concrete (PC) and crushing), 7 days and 6 months, were considered. The effect of RA's maturity is addressed in detail in a previous paper by the authors [12]. However, some results are repeated in this paper in order to analyse in detail the effect of reactive MgO. In this way, it is intended to provide a complete overview of the effect of MgO on the mechanical and shrinkage performance of recycled aggregate HPC.

2. Materials and methods

2.1. Raw materials

As indicated in the introduction, the developed mixes incorporated MgO and RA. The composition of HPC was completed with NA and ordinary Portland cement (OPC).

2.1.1. Binders, admixture, and water

Two different binders were used in this research work:

- On the one hand, all mixes were manufactured with OPC, CEM I 42.5 R (European standard), with a bulk and real density of around 1.0 and 3.1 Mg/m³, respectively. According to current regulations (EN 197-1 [32]), this type of cement has a clinker content of around 98%;
- On the other, in half of the mixes 10% OPC by weight was replaced with reactive MgO supplied by an Australian company. This commercial reactive MgO was characterized by its high purity (MgO content of 97%), as shown in the chemical composition obtained by X-ray fluorescence (XRF) analysis (Table 1). Moreover, it presented a high fineness as per its size gradation and surface area (Table 2), which allowed reaching its successful hydration, and therefore maximum expansion and strength development when mixed with

Table 1
Chemical composition (%) of reactive MgO by XRF.

MgO	CaO	SiO ₂	Fe ₂ O ₃	Al ₂ O ₃
97.0	1.3	1.2	0.2	0.3

Table 2
Properties of reactive MgO.

Real density (Mg/m^3)	3.58
Bulk density (Mg/m^3)	0.50
BET specific surface area (m^2/g)	60.21
Particles smaller than $75 \mu\text{m}$ (%)	100.00
Particles smaller than $45 \mu\text{m}$ (%)	95.00

water [44]. Finally, its higher real density and lower bulk density than OPC's can also be observed.

All mixes incorporated drinking water from the main water supply of Lisbon, Portugal, where the research was carried out. Moreover, a polycarboxylate-based superplasticiser specifically designed to provide concrete with high workability was also added.

2.1.2. Natural aggregates

Four natural aggregates (NA) with a continuous gradation (Fig. 1) and different sizes were used: crushed limestone gravels 12–22 mm (labelled coarse gravel, CG) and 4–12 mm (labelled medium gravel, MG), coarse siliceous sand 1–4 mm (labelled coarse sand, CS), and fine siliceous sand 0–1 mm (labelled fine sand, FS). Their physical properties had current values [45], as shown in Table 3.

2.1.3. Recycled aggregates

First, the composition and the slump of the parent concrete (PC) were defined (100% NA, Table 4) and its production was undertaken. The mechanical properties, as in Table 5, show that PC is classified as C30/37 class according to Eurocode 2 [1]. Furthermore, PC exhibited a fast development of strength: its 7-day compressive strength was equal to 87% of its compressive strength at 28 days. After its manufacture, PC was air cured for two different time periods: 7 days, when the shrinkage of concrete is still very high, and 6 months, when the shrinkage of concrete can be neglected. These two “maturities” allowed analysing the effect of the shrinkage of RA on the shrinkage of HPC. At the end of each curing period, PC was crushed in a jaw crusher and two types of RA were obtained: early-age (7-day air-curing period) and matured (6-month air-curing period).

Subsequently, RA obtained by crushing (0–31.5 mm) were sieved to separate their coarse (4–22 mm) and fine (0–4 mm) fractions. Thus, the ratio between the percentage of coarse (>4 mm) and fine (<4 mm) aggregate could be kept constant in all mixes, not affecting the results obtained [19].

Table 3 shows the main physical properties of RA. It can be noted that their density was around $2.4 \text{ Mg}/\text{m}^3$ and that their water absorption

Table 3
Density (Mg/m^3) and water absorption (%) of the aggregates (EN 1097-6 [46]).

Aggregate (size fraction)	Saturated-surface-dry density	Oven-dried density	Apparent density	24-h water absorption	10-min water absorption
CG (12–22 mm)	2.63	2.59	2.69	1.29	0.88
MG (4–12 mm)	2.65	2.62	2.70	1.11	0.85
CS (1–4 mm)	2.57	2.55	2.61	0.81	0.65
FS (0–1 mm)	2.62	2.61	2.65	0.62	0.39
Coarse RA (4–22 mm)	2.43	2.42	2.47	4.89	3.18
Fine RA (0–4 mm)	2.38	2.35	2.40	6.77	4.82

was four times higher for the coarse fraction and nine times higher for the fine fraction than those of NA, respectively, values in line with expectations [45]. Their gradation was also continuous (Fig. 2) and, therefore, suitable to produce HPC.

2.2. Mixes design

The reference mix, labelled RHPC, was first developed. The objective was to design a high-workability HPC (slump of $175 \pm 15 \text{ mm}$, i.e., S4 class as per EN 206 [47]), so that concrete had an optimal behaviour in both the fresh- and hardened-state. This ensured that it was a concrete suitable for structural use both in terms of strength and ease of placement [48]. To this end, three actions were implemented:

- A higher than usual OPC content, $400 \text{ kg}/\text{m}^3$, was adopted. Mineral additions, which are common in HPC [19], were not considered in order to avoid possible interactions that would have prevented a precise definition of the effect of RA or MgO;
- The ratio between the amount of aggregate and cement added to the mix was defined according to the specifications of Eurocode 2 [1]. The proportions of the four NA listed in section 2.1.2 were determined by adjusting by least squares their size fractions to the reference Faury's curve with a maximum aggregate size of 22 mm. Therefore, 55% coarse aggregate (35% CG and 20% MG) and 45% fine aggregate (20% CS and 25% FS) were added regarding the total volume of aggregates of the mix. In this way, a good packing of the aggregates was achieved;

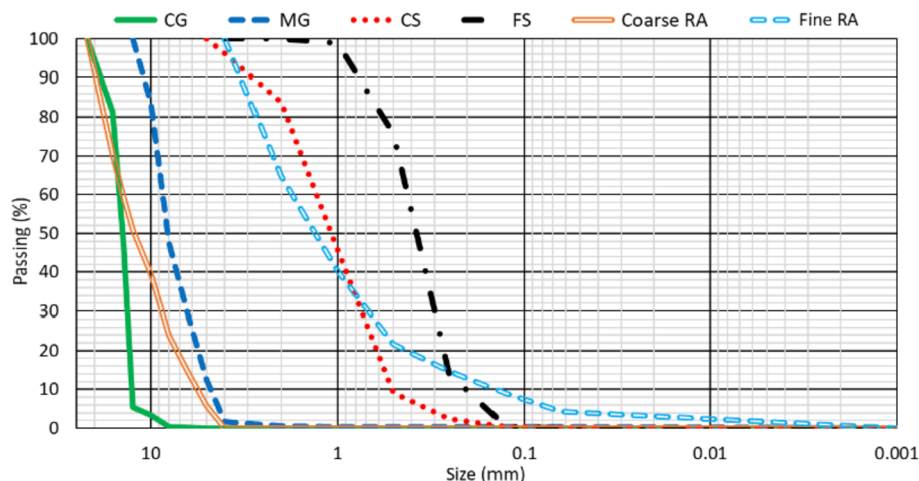


Fig. 1. Aggregates' gradation.

Table 4
Composition of PC (kg/m^3).

CEM I 52.5 R	Limestone filler	Water	CG	MG	CS	FS	Water-to-binder ratio	Slump (cm)
260	82	155	714	408	408	510	0.45	4.9 ± 0.2

Table 5
Mechanical properties of PC.

Compressive strength at 7 days (MPa)	39.70 ± 0.57
Compressive strength at 28 days (MPa)	45.50 ± 0.42
Splitting tensile strength at 28 days (MPa)	2.57 ± 0.29
Modulus of elasticity at 28 days (GPa)	37.30 ± 0.28

- A low effective water-to-binder (w/b) ratio, equal to 0.35, was established. For its definition, both the water absorption after 10 min (mixing time, section 2.3) and the natural moisture of NA, which were stored in the lab during the whole experiment, were considered. This low w/b ratio allowed obtaining a high strength, but reduced workability. The last problem was solved by adding a superplasticiser at a proportion of 2% cement mass and by implementing a two-stage mixing process (section 2.3).

Once the reference mix had been designed, the mixes with RA of different maturities were produced. So, 25% and 100% of the coarse and fine NA were simultaneously replaced with both matured and early-age RA. On the other hand, the water in each mix was adjusted to maintain the workability constant (slump of 175 ± 15 mm), thus ensuring that the water content did not affect the results obtained. The amount of additional water was empirically determined for each RA content according to the natural moisture of RA and their water absorption after 10 min. The mixes developed were labelled MAHPC25 and MAHPC100 (matured RA, labelled MA), and EAHPC25 and EAHPC100 (early-age RA, labelled EA).

Finally, five other mixes were defined, with an identical composition to the previous ones, but in which 10% by weight of OPC was replaced with MgO. This content of MgO was chosen because, in previous research regarding structural mortars, it had allowed an optimal balance between the decrease of shrinkage and the loss of strength that it causes [40]. Apart from studying the effect of MgO, through these mixes it was possible to study in detail its interaction with RA of different maturities. The water content of these five mixes was increased by $15 \text{ kg}/\text{m}^3$ to achieve the target slump (175 ± 15 mm). The five mixes with MgO were labelled RHPCMO, MAHPC25MO, MAHPC100MO, EAHPC25MO, and EAHPC100MO.

The composition of the ten HPC mixes produced is collected in Table 6, while their joint gradation is shown in Fig. 2. A correct packing of the aggregates can be observed. The moment of the production of each mix is shown on a time scale in Fig. 3.

2.3. Experimental plan

In order to maximize both the hydration of the cement and the water absorption of the aggregates [49] and, thus, the workability of the HPC, the mixing process was performed in two stages. In the first one, all the aggregates and 70% of the mixing water were added in a vertical-axis concrete mixer and mixed for four minutes. Subsequently, the mixer was stopped for two minutes, during which the binders (OPC and MgO) and the remaining water containing the superplasticiser were poured. The HPC was mixed for a further 4 min, after which the fresh-state tests were carried out:

- Two determinations of the slump, in accordance with the Abrams-cone test (EN 12350-2 [50]), with an interval of 1 min;
- Two measurements of the fresh density (EN 12350-6 [51]).

Subsequently, the necessary specimens to perform the different hardened-state tests were produced. These tests are listed in Table 7 along with the testing age and the type of specimen used in each case. All the tests were carried out on two specimens, so that the final result was the arithmetic mean of the values obtained for the individual specimens.

The specimens produced were stored in two conditions until the testing point:

- In general, the specimens were kept in a moist room ($95 \pm 5\%$ humidity and 20 ± 2 °C temperature);
- The specimens used to measure both hardened density and shrinkage were stored in a dry room ($45 \pm 5\%$ humidity and 20 ± 2 °C temperature).

Fig. 3 shows a flowchart that describes in detail the experimental plan followed, as well as the moment at which each mix was manufactured.

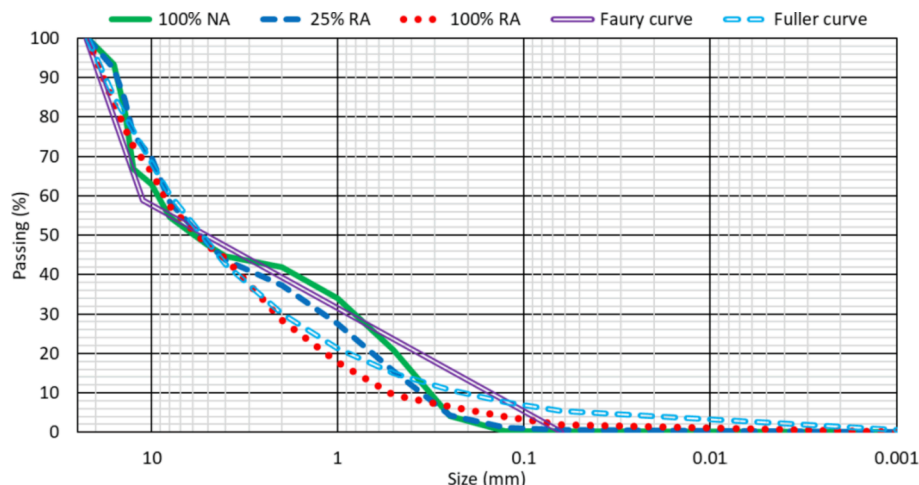


Fig. 2. Global gradation of the mixes.

Table 6
Mix design (kg/m³).

Mix	Cement	MgO	Water	CG	MG	CS	FS	Coarse RA	Fine RA	Superplasticiser
RHPC	400	0	150	690	390	380	470	0	0	8
MAHPC25	400	0	160	520	295	285	355	245	190	8
EAHPC25										
MAHPC100	400	0	195	0	0	0	0	980	760	8
EAHPC100										
RHPCMO	360	40	165	690	390	380	470	0	0	8
MAHPC25MO	360	40	175	520	295	285	355	245	190	8
EAHPC25MO										
MAHPC100MO	360	40	210	0	0	0	0	980	760	8
EAHPC100MO										

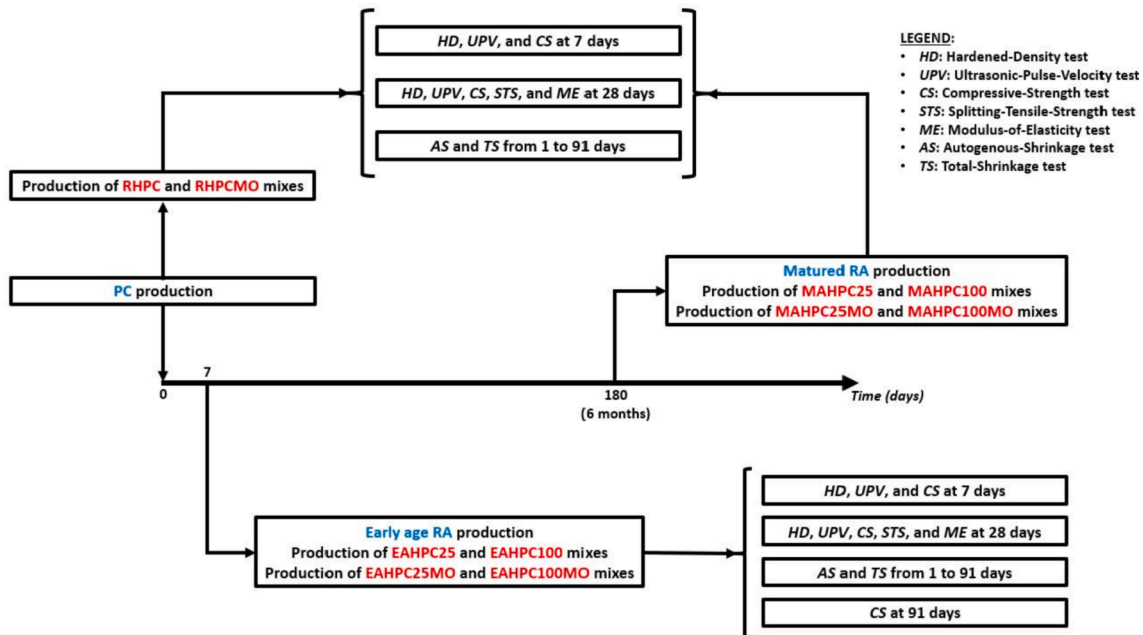


Fig. 3. Experimental plan.

Table 7
Hardened-state tests performed.

Test	Specimen type	Age (days)	Standard
Hardened density	10x10x10-cm cubic specimens	7, 28	EN 12390-7 [52]
Ultrasonic pulse velocity	15x15x15-cm cubic specimens	7, 28	EN 12504-4 [53]
Compressive strength	15x15x15-cm cubic specimens	7, 28, 91*	EN 12390-3 [54]
Splitting tensile strength	15x30-cm cylindrical specimens	28	EN 12390-6 [55]
Modulus of elasticity	15x30-cm cylindrical specimens	28	EN 12390-13 [56]
Autogenous shrinkage	10x10x50-cm prismatic specimens	From 1 to 91	-
Total shrinkage	10x10x50-cm prismatic specimens	From 1 to 91	LNEC-E398 [57]

* The 91-day compressive strength was determined only on the EA mixes to study the development of strength of early-age RA.

2.3.1. Shrinkage tests

In this research work, both autogenous and total shrinkage were measured in the same way, as per LNEC-E398 [57], and using a digital comparator, although the conditions of the specimens were different. The determination of total shrinkage was carried out on specimens that were in contact with the controlled environment (dry room), so water evaporation was enabled [58]. Regarding autogenous shrinkage, the

existing procedure for its short-term measurement (up to 2–3 days after the mixing process) was extended: the specimens were wrapped with aluminium foil tape to block water evaporation [59].

On the other hand, it has been indicated in the introduction that “time zero” is the moment when plastic shrinkage ends, and autogenous and drying shrinkage begin [7]. In high-performance cement pastes, this “time zero” is reached approximately 24 ± 0.5 h after the end of the mixing process [8]. Therefore, both types of shrinkage started to be measured at that time.

The number of measurements performed per week was in line with the shrinkage level expected at each age of concrete. As in similar studies [60], shrinkage was measured every day during the first week of the concrete’s life, three times in the second week, twice in the third and fourth weeks, and once per week until the concrete reached an age of 91 days, when the tests were ended. The ending age of the shrinkage tests was defined following the guidelines of other similar studies [58,61].

3. Results and discussion

3.1. Fresh properties

3.1.1. Workability

As shown in Table 8, all mixes had a slump within the initially established values, 175 ± 15 mm. Therefore, all mixes could be classified as S4 slump class as per EN 206 [47].

According to the results, it can be considered that workability

Table 8

Workability: w/b ratio and slump of the mixes.

Mix	w/b ratio	Effective w/b ratio	Slump (cm)	Δ RA content ¹ (%)	Δ RA's maturity ² (%)	Δ MgO ³ (%)
RHPC	0.373	0.350	18.55 ± 0.21	–	–	–
MAHPC25	0.400	0.354	18.10 ± 0.14	– 2.4	–	–
EAHPC25	0.400	0.354	18.33 ± 0.18	– 1.2	+ 1.3	–
MAHPC100	0.480	0.362	17.30 ± 0.13	– 6.7	–	–
EAHPC100	0.480	0.362	17.45 ± 0.14	– 5.9	+ 0.9	–
RHPCMO	0.408	0.385	17.85 ± 0.17	–	–	– 3.8
MAHPC25MO	0.435	0.389	17.40 ± 0.14	– 2.4	–	– 3.9
EAHPC25MO	0.435	0.389	17.30 ± 0.11	– 3.0	– 0.6	– 5.6
MAHPC100MO	0.515	0.397	16.15 ± 0.11	– 9.2	–	– 6.6
EAHPC100MO	0.515	0.397	16.30 ± 0.07	– 8.4	+ 0.9	– 6.7

¹ Percentage loss of slump because of the addition of RA (compared to the reference mixes with the same binders, RHPC or RHPCMO).

² Percentage variation caused by using early-age RA (compared to the mixes with the same composition but with matured RA).

³ Percentage decrease caused by MgO (regarding the mixes with the same composition and RA's maturity but with 100% OPC).

remained constant in all mixes. This was possible due to the increase in the effective w/b ratio when adding RA and MgO.

- The higher water absorption of RA than NA's [62] and the increase in friction between the mix components that the irregular shape of RA caused [19] were compensated by increasing the w/b ratio. The use of early-age RA increased the slump by around 1% due to their less angular shape as a result of the lower strength of PC when crushed;
- MgO has a greater specific surface area than OPC's [40], although both binders presented a similar size distribution, considering the specifications of EN 197-1 [32] and the data collected in Table 2. This led the effective w/b ratio to increase by 0.035 units when MgO was added to 100%-OPC mixes. Furthermore, the slightly more angular shape of MgO could also be detrimental [35].

Finally, Table 8 shows that RA caused a higher decrease of workability when they were added to a mix with MgO as cement replacement. This phenomenon was especially notable when 100% RA was used.

3.1.2. Fresh density

The fresh density of each HPC mix is shown in Fig. 4. The lower density of RA compared to NA's [63], as well as the increase of the w/b ratio and air content [64], led to a linear decrease of the fresh density when the RA content increased. On the other hand, the water evaporation that RA experienced during air curing [22] was higher in matured

RA than in early-age RA, due to their longer curing period. However, this loss of mass was very small compared to the joint mass of all components of HPC, so it did not affect the resulting fresh density.

The fresh density of the mixes manufactured with MgO was lower than that of the mixes that incorporated 100% OPC, although the real density of MgO is higher. This is explained by the higher water content when adding this binder, necessary to maintain the workability constant [35]. Furthermore, the higher specific surface area and more irregular shape of MgO could increase the air content of HPC, as other alternative binders [65]. This led the density of all mixes to decrease by around 0.02 Mg/m³ compared to the mixes with 100% OPC. The effect of MgO was always the same, regardless of the RA content of the mix or RA's maturity.

3.2. Hardened properties

3.2.1. Hardened density

The hardened density of the mixes is shown in Fig. 5. Common values for recycled aggregate concrete, between 2.15 and 2.45 Mg/m³, were obtained [66].

The replacement of 10% OPC with MgO decreased the hardened density, as observed regarding the fresh density. This was due to the higher water content required to maintain workability, which is less dense than the rest of components of concrete [40]. On the other hand, the addition of MgO also increases the porosity of concrete, which in

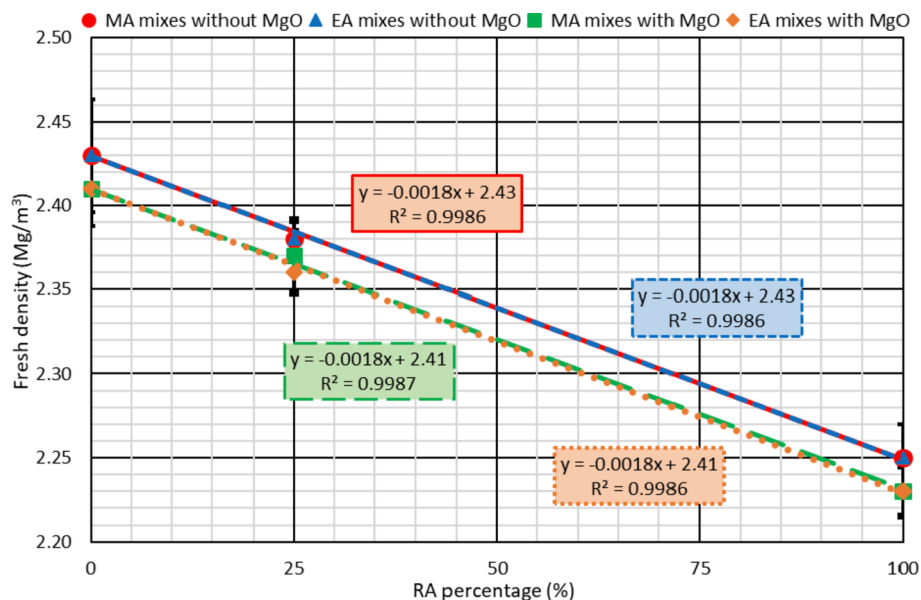


Fig. 4. Fresh density of HPC.

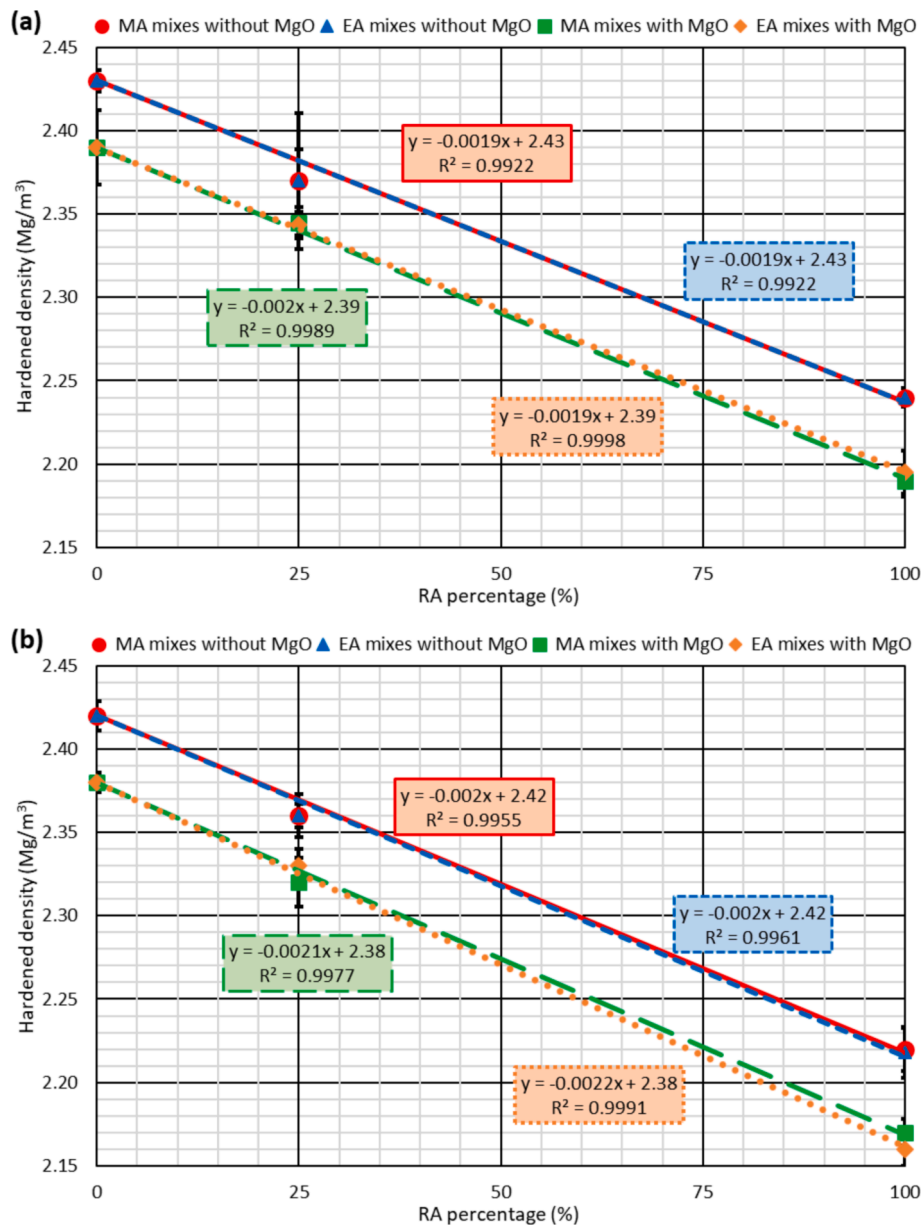


Fig. 5. Hardened density of HPC at (a) 7 days; (b) 28 days.

turn compensates the increase of microstructural density caused by the higher real density of MgO [67]. As a result of these two aspects, HPC with MgO had a hardened density 0.03–0.05 Mg/m³ lower than that of HPC with 100% OPC.

The lower density of RA compared to NA's, as well as the higher water and air content of HPC when adding these materials [63], decreased hardened density. This decrease showed a clear linear trend with the RA content, regardless of the binders used. On the other hand, there was a small variation of the hardened density between the mixes with the same amount of RA that incorporated MgO depending on the RA's maturity, although no clear trend was observed. These small variations were the common fluctuations of an experimental campaign, so it can be stated that the RA's maturity did not affect the hardened density of recycled aggregate HPC.

3.2.2. Compressive strength

The compressive strength of all mixes at both 7 and 28 days is shown in Fig. 6 and Table 9. The three factors analysed (RA content, RA's maturity, and addition of MgO) affected the compressive strength

obtained and its development over time.

On the one hand, compressive strength decreased linearly with the RA content (Fig. 6). This decrease was caused by the appearance of interfacial transition zones (ITZ) of bad quality between the coarser RA particles and the cementitious matrix [63] or the presence of mortar particles in the fine fraction [19]. The lower strength and stiffness of early-age RA [25] led to a greater loss of compressive strength.

Concerning MgO, its addition in a 10% by weight reduced the compressive strength of HPC by between 8% and 20% (Table 9). This phenomenon was due to the lower strength of the magnesium hydroxide (Mg(OH)₂), resulting from the hydration of the reactive MgO, compared to the calcium-silicate-hydrates (C-S-H), produced by the hydration of OPC [40]. Furthermore, the increase in water content when adding this binder resulted in a greater dilution of the cement and, therefore, in a loss of strength [43]. This loss of strength in HPC with 100% NA was similar to that obtained in similar researches [67].

The decrease of strength caused by MgO was higher when it was added to mixes made with RA, as shown in Table 9. Thus, the addition of MgO to the RHPC mix, resulting in the RHPCMO mix, reduced

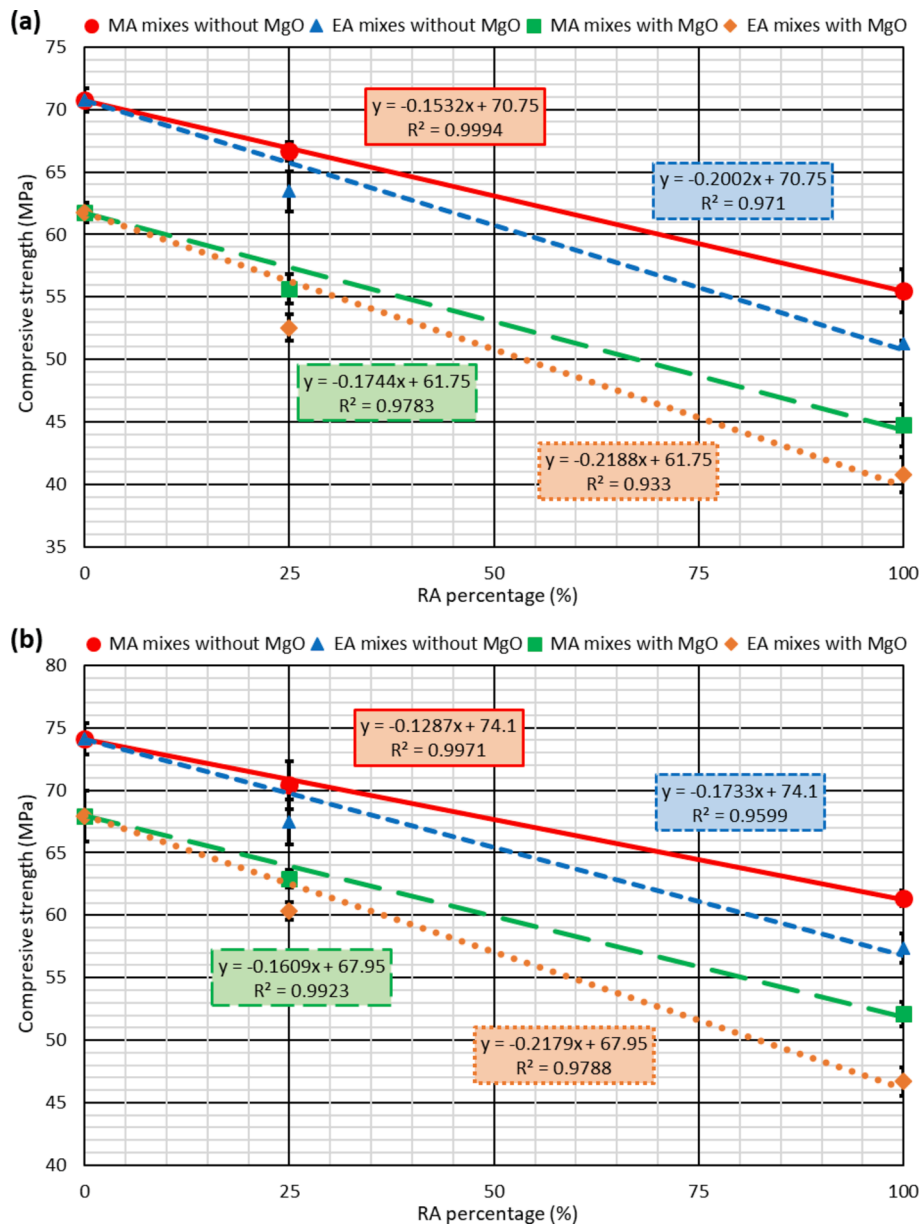


Fig. 6. Compressive strength of HPC at (a) 7 days; (b) 28 days.

Table 9
Effect of the factors on the compressive strength of HPC.

Mix	7 days	28 days			Δ 7–28 days ⁴ (%)	91 days Compressive strength (MPa)
	Compressive strength (MPa)	Compressive strength (MPa)	Δ RA content ¹ (%)	Δ RA's maturity ² (%)		
RHPC	70.8 ± 0.9	74.1 ± 1.3	–	–	–	–
MAHPC25	66.7 ± 0.8	70.4 ± 1.9	– 5.0	–	–	–
EAHPC25	63.5 ± 1.6	67.5 ± 1.8	– 9.0	– 4.2	–	–
MAHPC100	55.5 ± 1.7	61.4 ± 0.6	– 17.2	–	–	71.9 ± 1.6
EAHPC100	51.3 ± 0.2	57.4 ± 1.2	– 22.6	– 6.5	–	61.2 ± 1.8
RHPCMO	61.8 ± 0.8	68.0 ± 2.0	–	–	– 8.2	–
MAHPC25MO	55.7 ± 1.2	63.0 ± 0.7	– 7.4	–	– 10.5	–
EAHPC25MO	52.6 ± 1.1	60.4 ± 0.7	– 11.8	– 4.1	– 10.6	62.3 ± 2.4
MAHPC100MO	44.8 ± 1.7	52.1 ± 1.0	– 23.4	–	– 15.1	–
EAHPC100MO	40.8 ± 1.4	46.7 ± 1.1	– 31.3	– 10.4	– 18.6	50.6 ± 0.3

¹ Decrease of compressive strength due to the use of RA (compared to the reference mixes with the same binders, RHPC or RHPCMO).

² Percentage decrease because of using early-age RA (compared to the mixes with the same composition but with matured RA).

³ Percentage decrease caused by MgO (regarding the mixes with the same composition and RA's maturity but with 100% OPC).

⁴ Percentage of 28-day compressive strength developed at 7 days.

compressive strength by 8.2%, while its addition to the MAHPC100 and EAHPC100 mixes, resulting in the MAHPC100MO and EAHPC100MO mixes respectively, decreased it by 15–18%. This interaction, similar to that observed regarding slump (section 3.1.1), was attributed to the increase in porosity that the simultaneous use of both products caused, as observed with other alternative binders [68].

Finally, the temporal evolution of strength was different for each HPC mix, due to their different composition. On the one hand, the internal curing caused by RA due to their higher water absorption favoured a delayed hydration of the binders, and led to a higher increase of strength from 7 to 28 days [69]. On the other hand, the strength and stiffness of early-age RA increased more significantly over time [25], so that HPC produced with early-age RA showed a higher increase of compressive strength in the long-term. So, the 91-day compressive strength of the HPC with early-age RA was similar to the 28-day compressive strength of matured-RA HPC. Finally, as the evolution of compressive strength over time shows (seventh column of Table 9), the use of MgO also resulted in a higher temporal increase of strength, which could be due to the slower development of strength of MgO compared to OPC, as found in other alternative binders such as fly ash [70].

3.2.3. Splitting tensile strength

The splitting tensile strength of the different mixes at 28 days is shown in Fig. 7. Again, the three factors analysed, RA content, RA's maturity, and the presence of MgO, decreased strength, as the percentage variations in Table 10 show.

The addition of RA reduced the bond strength between the aggregates and the cementitious matrix [63] and, therefore, the splitting tensile strength of HPC. Early-age RA reduced the splitting tensile strength to a greater extent due to their lower strength [25]. Finally, the decrease of splitting tensile strength caused by 25% RA was higher than expected, regardless of RA's maturity, if a linear trend is considered (Fig. 7), which shows that the negative effect of RA on the splitting tensile strength is usually notable [48,63].

The replacement of 10% OPC with MgO reduced the splitting tensile strength by between 5 and 21%, very similar values to the decreases obtained for compressive strength. This decrease of splitting tensile strength was also caused by the greater dilution of OPC (due to the increase of the effective w/b ratio when MgO was added), the increase of porosity caused by the use of MgO, and the lower strength of Mg(OH)₂ compared to C-S-H [71]. In fact, the tensile strength of MgO is around 1

Table 10

Effect of the factors on the splitting tensile strength of HPC.

Mix	Splitting tensile strength (MPa)	Δ RA content ¹ (%)	Δ RA's maturity ² (%)	Δ MgO ³ (%)
RHPC	3.58 ± 0.15	–	–	–
MAHPC25	3.12 ± 0.10	– 12.8	–	–
EAHPC25	3.03 ± 0.12	– 15.4	– 2.9	–
MAHPC100	2.60 ± 0.09	– 27.4	–	–
EAHPC100	2.50 ± 0.13	– 30.2	– 3.8	–
RHPCMO	3.38 ± 0.09	–	–	– 5.6
MAHPC25MO	2.84 ± 0.11	– 16.0	–	– 9.0
EAHPC25MO	2.58 ± 0.09	– 23.7	– 9.2	– 14.9
MAHPC100MO	2.13 ± 0.18	– 37.0	–	– 18.1
EAHPC100MO	1.98 ± 0.07	– 41.4	– 7.0	– 20.8

¹ Decrease of strength due to the use of RA (compared to the reference mixes with the same binders, RHPC or RHPCMO).

² Percentage decrease because of using early-age RA (compared to the mixes with the same composition but with matured RA).

³ Percentage decrease caused by MgO (regarding the mixes with the same composition and RA's maturity but with 100% OPC).

MPa, while that of OPC is between 2 and 5 MPa [67]. In addition to the negative effect of MgO, its use amplified the negative effect on the splitting tensile strength of both the RA content and their maturity, as shown in Table 10. This phenomenon was also detected in compressive strength, but it was less relevant, possibly due to the greater dependence of the splitting tensile strength on the porosity of concrete [64], which increased because of the interaction between RA and MgO.

3.2.4. Modulus of elasticity

The use of RA reduces the modulus of elasticity of HPC due to their lower stiffness compared to NA's [25]. In addition, if RA are obtained from a lower quality concrete (lower strength and stiffness), this decrease is more remarkable [22]. Fig. 8 shows the values of the modulus of elasticity at 28 days of all mixes. The results were as expected. Thus, the modulus of elasticity decreased as the RA content rose. The use of early-age RA, obtained at an age at which PC had less stiffness, also reduced it, although this effect was only clear when its content was 100%.

Mg(OH)₂ has a similar modulus of elasticity to C-S-H's [40]. So, recent studies indicate that the replacement of OPC with MgO allow preserving the modulus of elasticity of cement-based materials, if this substitution does not imply any other change in the composition of the

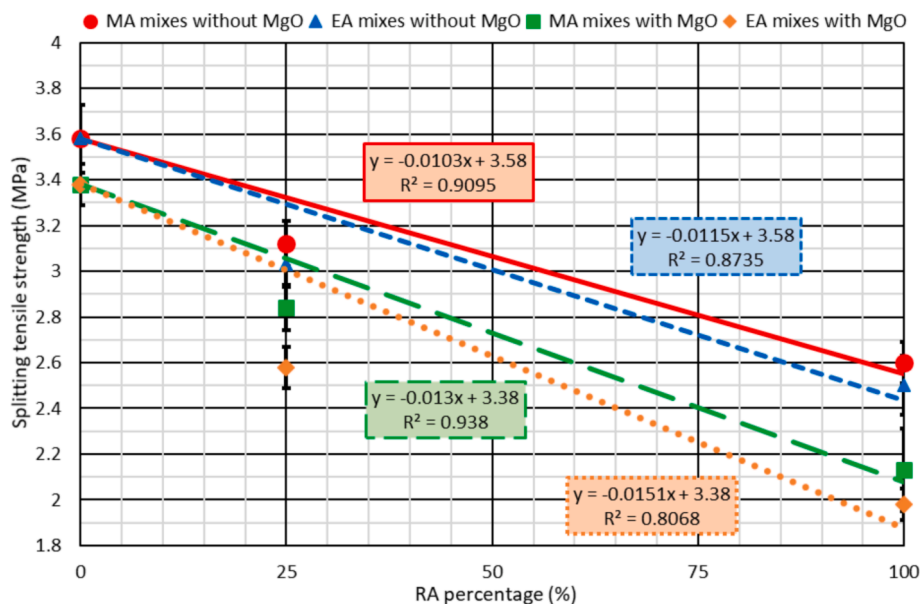


Fig. 7. Splitting tensile strength of HPC at 28 days.

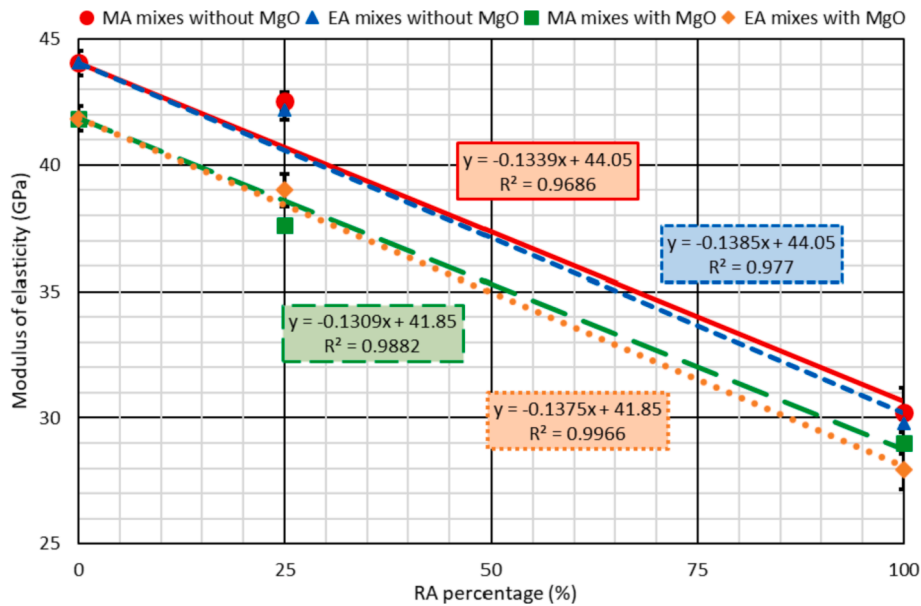


Fig. 8. Modulus of elasticity of HPC at 28 days.

mix [67]. However, the use of MgO forced an increase of water content to maintain workability, which also resulted in higher porosity of HPC [40]. Therefore, the elastic moduli of the mixes of this study decreased by around 5–10% when MgO was added, as shown in Table 11. However, this decrease was lower than those obtained for the compressive and splitting tensile strength. Furthermore, unlike those strengths, the relative decreases shown in Table 11 indicate that the effect of MgO was approximately the same in all mixes regardless of their RA content. Since microstructural density plays a very relevant role on the modulus of elasticity of HPC [14], its increase due to the higher real density of MgO compared to OPC's resulted in smaller and more uniform reduction of this mechanical property.

3.2.5. Ultrasonic pulse velocity (UPV)

UPV at the ages of 7 and 28 days of the mixes produced, measured in 15x15x15-cm cubic specimens subsequently tested to compressive strength, is shown in Fig. 9. All the values obtained, between 4000 and 5400 m/s, are typical of a high-stiffness concrete such as HPC [72].

UPV is closely related to the modulus of elasticity of concrete. Therefore, the behaviour of HPC regarding this property has many similarities with that regarding the modulus of elasticity:

- UPV decreased linearly with RA content, regardless of their maturity, due to the increase of porosity and the appearance of low-quality ITZ when this waste was added [48]. Furthermore, the lower stiffness of early-age RA compared to matured RA caused a slight decrease of UPV, more evident with the addition of 100% RA (Table 12);
- The use of MgO also reduced UPV around 4–6%, very similar values than those of the modulus of elasticity. Since Mg(OH)₂ and C-S-H have approximately the same stiffness [67], this effect was due to the higher dilution of the binder caused by the increase of the w/b ratio. Furthermore, the small increase in porosity caused by MgO could also favour these results;
- As in the modulus of elasticity, the percentage decrease of UPV when adding MgO was constant regardless of the amount and maturity of RA. Vice versa, the percentage decrease due to the content and maturity of RA was also constant regardless of the binder used. These aspects are clearly shown in Table 12.

Finally, in general, the internal curing caused by the delayed water release by the RA [63], as well as the slightly slower development of strength and stiffness of MgO compared to OPC, reduced the percentage of UPV developed at 7 days (Table 12). The increased stiffness over time of early-age RA had the same effect.

3.2.6. Statistical analysis

In previous sections, the effect of the different factors considered in this study (RA content, RA's maturity, and addition of MgO) has been described for each property. Moreover, it has been stated that the effect of MgO was not constant in both the compressive strength and the splitting tensile strength, but it was increasingly harmful as the RA content increased. These statements can be validated through a three-way ANalysis Of VAriance (ANOVA) for each property, which allows analysing the effect of each factor considering the effect of the others. The *p*-values obtained are shown in Table 13.

Considering a significance level of 5%, which is usual in this type of analysis, it can be stated that:

- The increase of RA content and the replacement of 10% OPC with MgO significantly affected all properties studied, *i.e.*, they always caused a notable decrease of the property analysed. However, the maturity of RA was only significant in compressive strength, which

Table 11

Effect of the factors on the modulus of elasticity of HPC.

Mix	Modulus of elasticity (GPa)	Δ RA content ¹ (%)	Δ RA's maturity ² (%)	Δ MgO ³ (%)
RHPC	44.1 ± 0.5	–	–	–
MAHPC25	42.6 ± 0.4	– 3.4	–	–
EAHPC25	42.2 ± 0.4	– 4.3	– 0.9	–
MAHPC100	30.2 ± 1.0	– 31.6	–	–
EAHPC100	29.8 ± 0.2	– 32.4	– 1.3	–
RHPCMO	41.8 ± 0.5	–	–	– 5.2
MAHPC25MO	37.6 ± 0.2	– 10.0	–	– 11.7
EAHPC25MO	39.0 ± 0.6	– 6.7	+ 3.7	– 7.6
MAHPC100MO	29.0 ± 0.4	– 30.6	–	– 4.0
EAHPC100MO	27.9 ± 0.8	– 33.3	– 3.8	– 6.4

¹ Decrease in percentage due to the use of RA (compared to the reference mixes with the same binders, RHPC or RHPCMO).

² Percentage variation because of using early-age RA (compared to the mixes with the same composition but with matured RA).

³ Percentage decrease caused by MgO (regarding the mixes with the same composition and RA's maturity but with 100% OPC).

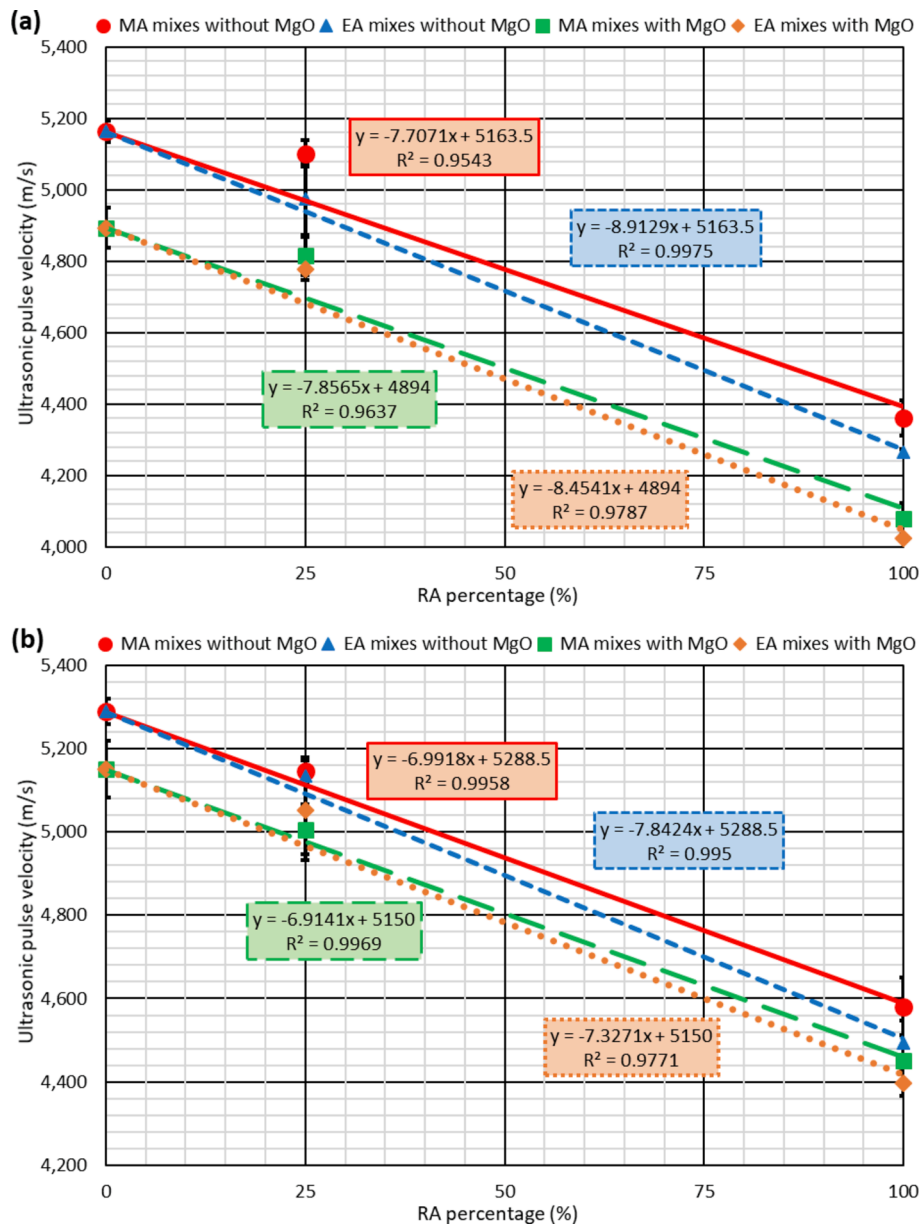


Fig. 9. UPV of HPC at (a) 7 days; (b) 28 days.

Table 12
Effect of the factors on the UPV of HPC.

Mix	7 days	28 days			Δ 7–28 days ⁴ (%)
	UPV (m/s)	UPV (m/s)	Δ RA content ¹ (%)	Δ RA's maturity ² (%)	
RHPC	5163 ± 30.4	5289 ± 30.4	–	–	97.6
MAHPC25	5102 ± 30.1	5147 ± 31.1	– 1.2	–	99.1
EAHPC25	4974 ± 101.1	5134 ± 10.1	– 3.7	– 2.5	96.9
MAHPC100	4360 ± 49.5	4581 ± 69.3	– 15.6	–	95.2
EAHPC100	4264 ± 9.9	4494 ± 52.3	– 17.4	– 2.2	94.9
RHPCMO	4894 ± 56.6	5150 ± 67.9	–	–	95.0
MAHPC25MO	4815 ± 53.7	5006 ± 60.1	– 1.6	–	96.2
EAHPC25MO	4777 ± 28.3	5052 ± 120.2	– 2.4	+ 0.8	94.6
MAHPC100MO	4079 ± 43.8	4452 ± 30.4	– 16.7	–	91.6
EAHPC100MO	4025 ± 42.4	4396 ± 30.4	– 17.8	– 1.3	91.6

¹ Decrease of UPV due to the use of RA (compared to the reference mixes with the same binders, RHPC or RHPCMO).

² Percentage decrease because of using early-age RA (compared to the mixes with the same composition but with matured RA).

³ Percentage decrease caused by MgO (regarding the mixes with the same composition and RA's maturity but with 100% OPC).

⁴ Percentage of 28-day UPV developed at 7 days.

Table 13
P-values of the three-way ANOVA for the fresh and mechanical properties of HPC.

Property	RA content ¹	RA's maturity ¹	MgO ¹	RA content – RA's maturity ²	RA content – MgO ²	RA's maturity – MgO ²
Slump	0.0044	0.3224	0.0037	0.6160	0.1490	0.4226
Fresh density	0.0002	0.4226	0.0082	0.5000	0.5000	0.4226
7-day hardened density	0.0002	1.0000	0.0014	0.5000	0.0577	1.0000
28-day hardened density	0.0004	0.9002	0.0036	0.3921	0.1719	0.9002
7-day compressive strength	0.0000	0.0002	0.0000	0.0009	0.0036	0.2495
28-day compressive strength	0.0007	0.0113	0.0012	0.0370	0.0333	0.5799
Splitting tensile strength	0.0014	0.0581	0.0051	0.1902	0.0403	0.2832
Modulus of elasticity	0.0018	0.8696	0.0185	0.4944	0.1808	0.6598
7-day UPV	0.0006	0.0563	0.0026	0.1960	0.7205	0.2333
28-day UPV	0.0004	0.1698	0.0051	0.0938	0.5008	0.2204

¹ Effect of each factor.
² Second-order interactions.

shows that the strength of RA seems to have a greater relevance to the mechanical behaviour of HPC than their stiffness;

- Second-order interactions between the factors only occurred for compressive strength and splitting tensile strength. For compressive strength, the negative effect caused by early-age RA was more detrimental the higher the RA content of the mix (RA content-RA's maturity interaction). This may be because the effect of RA's

maturity was significant on this strength. On the other hand, the effect of MgO was also more harmful the greater the RA amount (RA content-MgO interaction) regarding compressive strength and splitting tensile strength. Finally, the effect of RA's maturity was always the same regardless of the binder used (RA's maturity-MgO interaction).

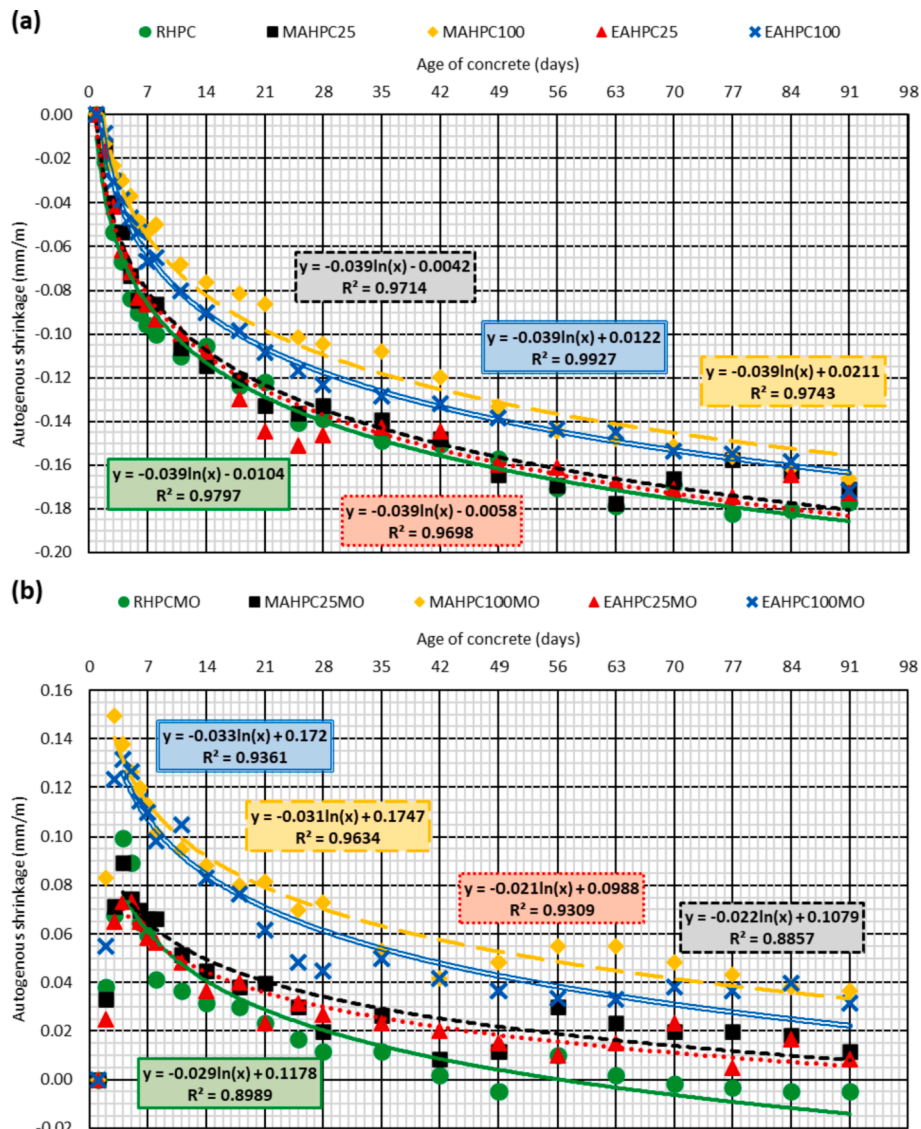


Fig. 10. Autogenous shrinkage of HPC mixes: (a) without MgO; (b) with 10% MgO.

3.3. Shrinkage behaviour

3.3.1. Autogenous shrinkage

Autogenous shrinkage is caused by the consumption of capillary water due to the chemical reaction that occurs during the delayed hydration of cement [15], i.e., the hydration of cement after a stable skeleton is formed into the concrete (point known as “time zero”) [8]. In the mixes of this study, this type of shrinkage was measured in 10x10x50-cm prismatic specimens, wrapped with aluminium foil tape in order to block water evaporation. The results obtained are shown in Fig. 10, while Table 14 shows the effect of each factor (RA content, RA’s maturity, and presence of MgO).

Fig. 10a shows that using RA reduced autogenous shrinkage due to its higher water storage capacity than NA’s [10]. Therefore, their higher release of water during the deferred hydration of cement allowed more efficiently replacing the water consumed during this process [22]. Furthermore, this phenomenon compensated their lower resistance to the contraction of the cementitious matrix due to their higher deformability [58]. Early-age RA shrink due to their rheological nature, so their use increased the autogenous shrinkage. Their lower stiffness could also favour this situation.

As explained in the introduction, reactive MgO is expansive, since the resulting Mg(OH)₂ after its hydration has a larger volume than MgO [27]. This quality allows using this product as shrinkage-reducing agent in cement-based materials [39], as recently demonstrated in mortars [40]. Fig. 10b demonstrates that the reactive MgO was also a suitable autogenous-shrinkage-reducing agent in HPC, so that the replacement of 10% OPC with MgO led to a decrease of autogenous shrinkage of 93% in the reference mix. Concerning its joint use with matured RA, the decrease of the autogenous shrinkage caused by using MgO, compared to a HPC with the same RA amount but with 100% OPC, was greater the higher the matured RA content (Table 14). In this way, the shrinkage reduction when increasing the amount of RA was higher in the mixes with MgO rather than 100% OPC. This situation is evident in the MAHPC25MO mix, which presented a notably lower autogenous shrinkage than the RHPCMO mix, unlike that found in the mixes without MgO, in which the effect of adding 25% matured RA was minimal. This behaviour can be explained by two different aspects:

- Firstly, the lower stiffness of RA compared to NA [21] meant that they exhibited lower opposition to the expansion of MgO;
- Secondly, the higher ability of RA to store water and release it in a deferred way [11] allowed a higher percentage of MgO particles that did not hydrate during the mixing process to do so later. A larger quantity of hydrated MgO particles led to a higher expansion and, in

turn, to a greater opposition to the contraction of the cementitious matrix.

Considering these aspects, the effect of MgO in the mixes with early-age RA should have been higher due to their lower stiffness. However, the shrinkage of early-age RA had a higher relevance than their stiffness and, therefore, the autogenous shrinkage increased when early-age RA were used. Despite this, no mix made with RA experienced autogenous shrinkage during the test period, since their final length at 91 days was greater than their initial length at 1 day. The greatest length increase was in the MAHPC100MO mix (0.035 mm/m at 91 days), which is in line with all the aspects commented on.

Fig. 10b also shows that the expansion of MgO mostly occurs during the first days, since most of the MgO was hydrated during the mixing process. However, no precise pattern was detected regarding the time during which the HPC increased in length. Thus, the RHPCMO and MAHPC100MO mixes expanded for two days, while the rest of the mixes expanded for three days. This aspect seems to be linked to the efficiency of the hydration of MgO during the mixing process [49], so the composition of concrete has no relevant role. Therefore, the presence of RA did not influence the initial hydration and subsequent expansion of MgO, although it was relevant in the long-term hydration of MgO, as indicated above.

Finally, it can be stated according to Fig. 10b that the evolution of autogenous shrinkage over time in HPC with MgO follows a logarithmic function, as found in conventional concrete [10] and HPC with 100% OPC (Fig. 10a). In fact, it is possible to precisely adjust this type of function to mixes with this composition as long as the values during the first days (from the first to the fourth day approximately) are not considered, as most of the expansion of MgO occurs during those days.

3.3.2. Drying shrinkage

Drying shrinkage is produced by the evaporation of water from concrete after “time zero” [9]. This type of shrinkage may not be measured directly, as this phenomenon cannot be empirically separated from autogenous shrinkage. Therefore, the most suitable method to determine it is to calculate the difference between the shrinkage of non-wrapped specimens and that of specimens wrapped with aluminium foil tape. In this way, autogenous shrinkage is subtracted from total shrinkage and, thus, drying shrinkage is isolated [1]. Drying shrinkage of the mixes is shown in Fig. 11, while the effect of each factor is detailed in Table 15.

As shown in Fig. 11, the effect of increasing the RA content and using MgO on drying shrinkage was exactly the opposite to that on autogenous shrinkage: they did not reduce drying shrinkage, but increased it instead. This was attributed to the necessary increment in the w/b ratio to maintain the workability constant [26].

Table 14

Effect of the factors on autogenous shrinkage of HPC at 91 days.

Mix	Autogenous shrinkage (mm/m)	Δ RA content ¹ (%)	Δ RA’s maturity ² (%)	Δ MgO ³ (%)
RHPC	-0.186 ± 0.013	-	-	-
MAHPC25	-0.180 ± 0.025	-3.2	-	-
EAHPC25	-0.182 ± 0.012	-2.2	+1.1	-
MAHPC100	-0.155 ± 0.029	-16.7	-	-
EAHPC100	-0.164 ± 0.030	-11.8	+5.8	-
RHPCMO	-0.013 ± 0.040	-	-	-93.0
MAHPC25MO	+0.009 ± 0.016	-169.2	-	-105.0
EAHPC25MO	+0.004 ± 0.043	-130.8	+55.6	-102.2
MAHPC100MO	+0.035 ± 0.009	-369.2	-	-122.6
EAHPC100MO	+0.023 ± 0.012	-276.9	+34.3	-114.0

¹ Percentage variation due to the use of RA (compared to the reference mixes with the same binders, RHPC or RHPCMO).

² Percentage variation of using early-age RA (compared to the mixes with the same composition but with matured RA).

³ Variation in percentage caused by MgO (regarding the mixes with the same composition and RA’s maturity but with 100% OPC).

- The higher delayed release of water of RA increased the available water to evaporate, which in turn increased the drying shrinkage of HPC [22]. This phenomenon was also favoured by the lower stiffness of RA [58];
- The higher specific surface area of MgO compared to OPC meant that the water content of HPC had to be increased to retain workability when replacing OPC with MgO [35]. Thus, the water available for evaporation was higher [21], which led drying shrinkage to increase in the mixes made with 90% OPC and 10% MgO compared to the mixes with the same composition but 100% OPC (Table 15). The contraction caused by water evaporation was greater than the expansion of MgO, so no length increase was detected, as shown in Fig. 11b.

RA’s maturity had the same effect as on autogenous shrinkage, as the shrinkage of early-age RA and their lower stiffness resulted in increased drying shrinkage. This increase was more pronounced when adding small quantities of RA (Table 15), so the increase of drying shrinkage

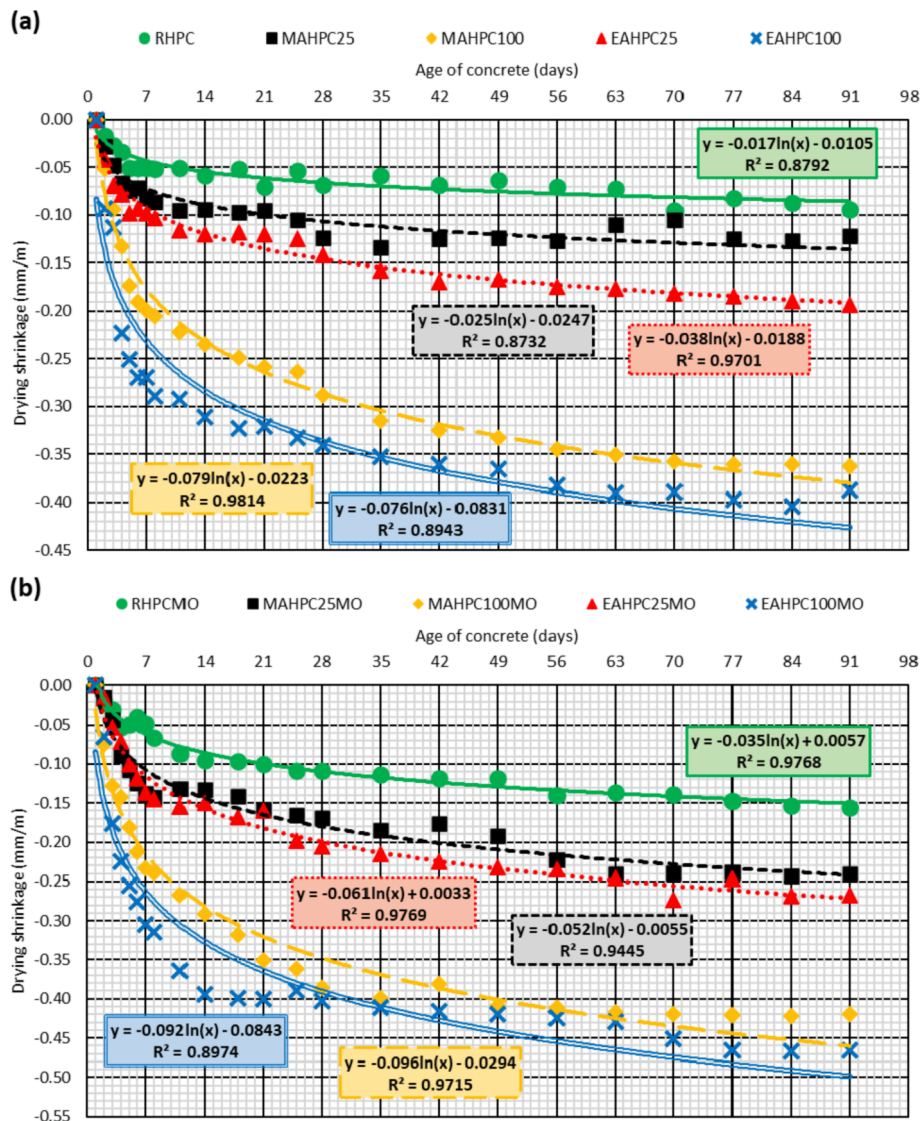


Fig. 11. Drying shrinkage of HPC mixes: (a) without MgO; (b) with 10% MgO.

Table 15
Effect of the factors on drying shrinkage of HPC at 91 days.

Mix	Drying shrinkage (mm/m)	Δ RA content ¹ (%)	Δ RA's maturity ² (%)	Δ MgO ³ (%)
RHPC	-0.087 ± 0.026	-	-	-
MAHPC25	-0.137 ± 0.037	+ 57.5	-	-
EAHPC25	-0.190 ± 0.046	+ 118.4	+ 38.7	-
MAHPC100	-0.379 ± 0.035	+ 335.6	-	-
EAHPC100	-0.426 ± 0.006	+ 389.7	+ 12.4	-
RHPCMO	-0.152 ± 0.007	-	-	+ 74.7
MAHPC25MO	-0.240 ± 0.035	+ 57.9	-	+ 75.2
EAHPC25MO	-0.272 ± 0.023	+ 78.9	+ 13.3	+ 43.2
MAHPC100MO	-0.462 ± 0.019	+ 203.9	-	+ 21.9
EAHPC100MO	-0.499 ± 0.024	+ 228.3	+ 8.0	+ 17.1

¹ Percentage variation due to the use of RA (compared to the reference mixes with the same binders, RHPC or RHPCMO).

² Percentage variation of using early-age RA (compared to the mixes with the same composition but with matured RA).

³ Variation in percentage caused by MgO (regarding the mixes with the same composition and RA's maturity but with 100% OPC).

was mainly due to the higher water content of HPC when adding large quantities of RA, so the shrinkage of early-age RA played a secondary role.

Finally, Table 15 also shows that the relative increase of drying shrinkage due to the addition of MgO decreased as the RA content of HPC increased. This is explained because the increment of drying shrinkage caused by MgO was very similar in all mixes, which resulted in this shrinkage increase having less relevance in mixes made with large amounts of RA, due to their higher drying shrinkage [11]. Furthermore, although MgO expansion could not be perceived by the naked eye in the drying-shrinkage curves, it occurred and could be slightly higher in HPC with RA, as in autogenous shrinkage, which could also favour this performance [40].

3.3.3. Total shrinkage

Total shrinkage is the type of shrinkage that can be most easily determined, as it is measured on non-wrapped specimens that are directly in contact with the environment [23]. Since water evaporation is allowed and the phenomena that cause autogenous shrinkage occur simultaneously, the value obtained is the sum of autogenous and drying shrinkage [1]. The total shrinkage of the HPC mixes developed is shown in Fig. 12, while the percentage variations caused by each factor are listed in Table 16.

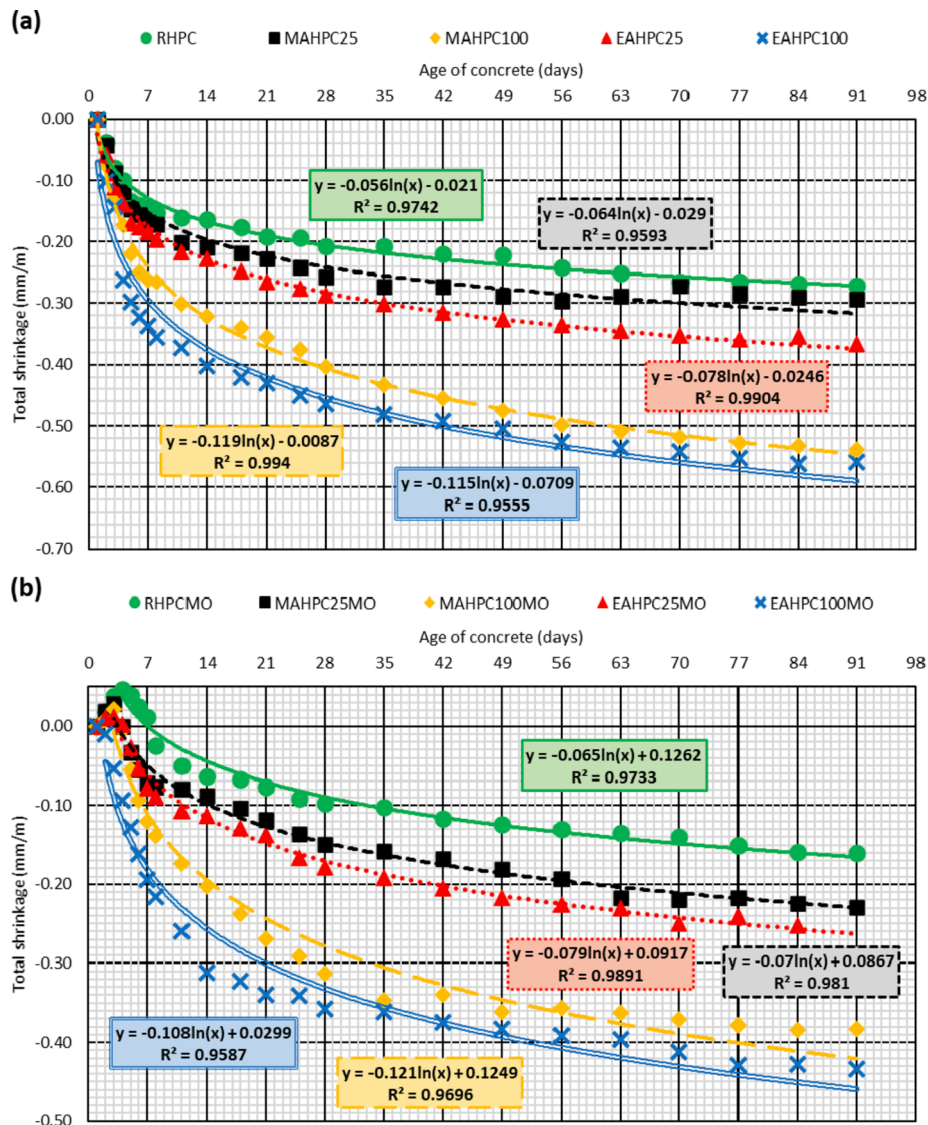


Fig. 12. Total shrinkage of HPC mixes: (a) without MgO; (b) with 10% MgO.

Table 16
Effect of the factors on total shrinkage of HPC at 91 days.

Mix	Total shrinkage (mm/m)	Δ RA content ¹ (%)	Δ RA's maturity ² (%)	Δ MgO ³ (%)
RHPC	-0.274 ± 0.022	-	-	-
MAHPC25	-0.318 ± 0.012	+ 16.1	-	-
EAHPC25	-0.376 ± 0.026	+ 37.2	+ 18.2	-
MAHPC100	-0.545 ± 0.007	+ 98.9	-	-
EAHPC100	-0.590 ± 0.011	+ 115.3	+ 8.3	-
RHPCMO	-0.167 ± 0.033	-	-	- 39.1
MAHPC25MO	-0.229 ± 0.018	+ 37.1	-	- 28.0
EAHPC25MO	-0.265 ± 0.027	+ 58.7	+ 15.7	- 29.5
MAHPC100MO	-0.421 ± 0.028	+ 152.1	-	- 22.8
EAHPC100MO	-0.457 ± 0.036	+ 173.7	+ 8.6	- 22.5

¹ Percentage variation due to the use of RA (compared to the reference mixes with the same binders, RHPC or RHPCMO).

² Percentage variation of using early-age RA (compared to the mixes with the same composition but with matured RA).

³ Variation in percentage caused by MgO (regarding the mixes with the same composition and RA's maturity but with 100% OPC).

In summary, the effect on total shrinkage of each change in the composition of HPC is the sum of the effects detected in both autogenous and drying shrinkage [1]. Furthermore, drying shrinkage has a greater magnitude, so that total shrinkage mainly depends on it [9]. In this way, drying shrinkage and total shrinkage usually exhibit similar trends [39]. However, in the present study, this was only fulfilled for two of the three factors analysed:

- The RA content and the use of early-age RA had the same effect as on drying shrinkage. Thus, the higher the amount of RA, the greater the total shrinkage, due to their higher deformability and water absorption [58]. Furthermore, the lower stiffness of early-age RA compared to matured RA and their shrinkage also increased the total shrinkage of HPC;
- On the other hand, the use of MgO reduced the total shrinkage of HPC, even though its use increased drying shrinkage, as was also observed in mortars [40]. This was because the decrease of autogenous shrinkage was much greater than the increase of drying shrinkage caused by the increment of the water content to retain workability [39]. In line with this, the length increase of the specimens during the first days, due to MgO expansion, was explicitly reflected in the total-shrinkage curves (Fig. 12b), although no clear trend could be detected regarding the expansion time, as in

autogenous shrinkage. Therefore, it could be concluded that the effect of MgO in HPC is fundamentally conditioned by autogenous shrinkage, unlike what happens to OPC.

As the effect of RA and MgO were opposite regarding the total shrinkage, when using them both it could be observed that the percentage reduction of total shrinkage caused by MgO decreased as the RA content of HPC increased (Table 16). The increment of drying shrinkage caused by RA was much higher than the decrease of autogenous shrinkage caused by MgO, as shown in Table 14 and Table 15. Therefore, the effectiveness of MgO as total-shrinkage-reducing agent was higher in HPC made with NA. In this way, the addition of more than 42% matured RA compensated for the reduction in total shrinkage caused by MgO, as shown in Fig. 13. This content was lower for early-age RA (35%) due to their shrinkage and lower stiffness.

3.3.4. Statistical analysis

To provide a solid basis for the statements of previous sections [63] regarding the effect of the RA content and their maturity, as well as the use of MgO, the p-values of the three-way ANOVA conducted with the

Table 17

P-values for the three-way ANOVA for the different shrinkage types at 91 days.

Type of shrinkage	Autogenous	Drying	Total
RA content ¹	0.0006	0.0002	0.0004
RA's maturity ¹	0.0113	0.0114	0.0118
MgO ¹	0.0000	0.0015	0.0008
RA content – RA's maturity ²	0.0256	0.0443	0.0550
RA content – MgO ²	0.0099	0.0272	0.1218
RA's maturity – MgO ²	0.1835	0.2305	0.2470

¹ Effect of each factor.

² Second-order interactions.

values at 91 days of the different shrinkage types analysed are provided in Table 17.

Considering a significance level of 5% (95% confidence level), it can be stated that:

- The three factors evaluated (RA content, RA's maturity, and replacement of 10% OPC with MgO) significantly influenced all

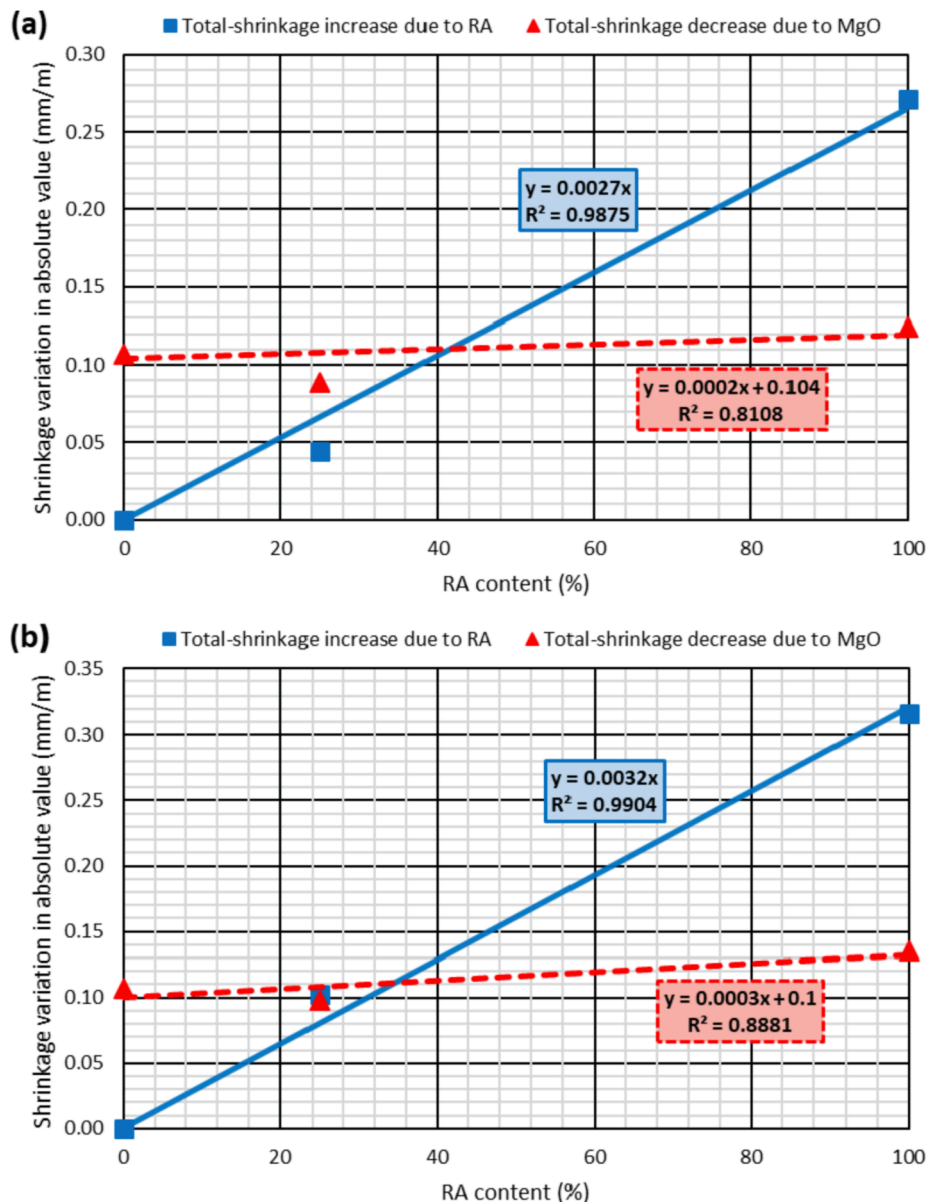


Fig. 13. Comparison of shrinkage variations caused by RA and MgO: (a) matured RA; (b) early-age RA.

shrinkage types, which means that any modification in them led to perceptible changes in every type of shrinkage of HPC;

- The second-order interaction between RA content and RA's maturity was significant in the autogenous and drying shrinkage. As indicated in previous sections, the increase of shrinkage of HPC caused by early-age RA depended on their content. This effect was negligible in total shrinkage because the low increase of this shrinkage that early-age RA produced in HPC when increasing RA content was very small compared to the high shrinkage levels of HPC;
- The effect of MgO in autogenous and drying shrinkage depended on the RA content of HPC. Thus, both the lower stiffness of RA compared to NA and its higher delayed water release increased the expansion of MgO and the reduction of these types of shrinkage. This interaction was not significant in total shrinkage either;
- Finally, the effect of MgO did not depend on RA's maturity. Thus, the slightly greater expansion of MgO when using early-age RA due to their lower stiffness compared to matured RA was offset by the shrinkage of early-age RA.

4. Conclusions

This article has studied the effect of replacing ordinary Portland cement (OPC) with reactive magnesium oxide (MgO) on the mechanical and shrinkage behaviour of high-performance concrete (HPC). In addition, the interaction of MgO with different contents of Recycled Aggregates (RA) of different maturities has also been analysed. For this purpose, ten HPC mixes were produced with 0%, 25%, and 100% RA of two different maturities: after a 7-day air curing of the parent concrete (PC), called early-age RA, and after a 6-month air curing of the PC, called matured RA. Half of the mixtures were manufactured with 100% OPC, while in the other half 10% OPC was replaced with reactive MgO. From the discussions throughout the article, the following conclusions can be drawn:

- The higher specific surface area of MgO compared to OPC, as well as its more irregular shape, required increasing the water-to-binder (w/b) ratio of the HPC to maintain workability. This increase of the water content also reduced both the fresh and hardened density of HPC, despite the higher real density of MgO than OPC;
- Mg(OH)₂ produced during the hydration of MgO has lower strength than the calcium-silicate-hydrates generated in the hydration of OPC. Furthermore, the necessary increase of the w/b ratio when using MgO resulted in a greater dilution of the binder. These two aspects decreased the compressive strength, splitting tensile strength, modulus of elasticity, and ultrasonic pulse velocity by 5–8% when 10% OPC was replaced with MgO. The addition of RA also worsened the mechanical behaviour of HPC, and the effect of RA was more harmful the higher their content and the lower their strength and stiffness (early-age RA). Interaction between the RA content and the presence of MgO was detected in compressive strength and splitting tensile strength, so that the corresponding negative effects were amplified when these materials were used simultaneously (decreases of 19–21% in HPC with 100% RA when adding MgO);
- The improved capacity of RA to store water and release it in a delayed way compared to NA decreased the autogenous shrinkage of HPC by replacing more effectively the capillary water consumed during the deferred hydration of binder. However, this also increased the amount of water available to evaporate, which in turn increased drying shrinkage. The higher value of drying shrinkage caused total shrinkage to show the same trend, so it grew when the RA content of HPC increased. For 100% matured RA, autogenous shrinkage decreased by 17%, while drying and total shrinkage increased by 336% and 99%, respectively. The lower stiffness of early-age RA, as well as their shrinkage, led to an increase of all shrinkage types;

- The expansion caused by the formation of Mg(OH)₂ during the hydration of reactive MgO led to a decrease of autogenous shrinkage of 93%, so that autogenous shrinkage when replacing 10% OPC with MgO was minimal or not at all. However, the higher water content of HPC with MgO increased drying shrinkage by 75%. Finally, total shrinkage decreased 39% when using MgO, which shows that the decrease of autogenous shrinkage exceeded the increase of drying shrinkage. Therefore, MgO proved to be a suitable shrinkage-reducing agent in HPC;
- The percentage decrease of autogenous shrinkage due to MgO increased with the RA content of HPC. Likewise, the percentage increase of drying shrinkage caused by MgO was lower when the RA content rose. This behaviour occurred because the expansion of MgO was favoured by the lower stiffness of RA and by their delayed water release, which allowed the hydration of a greater amount of MgO particles and, in turn, a greater expansion. However, the increase of the RA content in HPC with MgO reduced the effectiveness of the expansion of this product, so that the increase of drying shrinkage caused by RA was higher than the decrease of autogenous shrinkage caused by MgO. Thus, the reduction of total shrinkage caused by MgO was 28% in HPC with 25% RA, and 22% when 100% RA was added.

Overall, it can be concluded that MgO was a binder that added at 10% of the total content of binder effectively reduced the shrinkage of HPC, while the decrease of mechanical properties it caused was reasonable. However, its effectiveness as shrinkage-reducing agent was lower when it was used simultaneously with RA. In fact, for contents above 42% matured RA, and 35% early-age RA, the increase of total shrinkage caused by RA was greater than the shrinkage reduction due to MgO.

Declaration of Competing Interest

The authors declare that they have no known competing financial interests or personal relationships that could have appeared to influence the work reported in this paper.

Acknowledgements

This work was supported by the Spanish Ministry of Universities, MICINN, AEI and ERDF [grant numbers FPU17/03374; EST19/00263; PID2020-113837RB-I00; 10.13039/501100011033]. The authors also acknowledge the support of the Foundation for Science and Technology, CERIS Research Centre and Instituto Superior Técnico, the Junta de Castilla y León [grant number UIC231], and the University of Burgos [grant number Y135.GI].

References

- [1] EC2, Eurocode 2: Design of concrete structures. Part 1-1: General rules and rules for buildings, CEN (European Committee for Standardization) (2010).
- [2] J. Nam, G. Kim, J. Yoo, G. Choe, H. Kim, H. Choi, Y. Kim, Effectiveness of fiber reinforcement on the mechanical properties and shrinkage cracking of recycled fine aggregate concrete, *Materials* 9 (3) (2016) 131.
- [3] X. Wu, J. Zhou, T. Kang, F. Wang, X. Ding, S. Wang, Laboratory investigation on the shrinkage cracking of waste fiber-reinforced recycled aggregate concrete, *Materials* 12 (8) (2019) 1196.
- [4] J. Torres, C. Andrade, J. Sánchez, Initiation period of corrosion by chloride ion according to EHE 08 in cracked concrete elements, *Inf. Constr.* 72 (557) (2020), e331.
- [5] P. Anaya, J. Rodríguez, C. Andrade, B. Martín-Pérez, C.L. Hombrados, Determination of wires transfer length in prestressed concrete members with different levels of corrosion, *Inf. Constr.* 72 (558) (2020), e339.
- [6] N. Bantia, R. Gupta, Influence of polypropylene fiber geometry on plastic shrinkage cracking in concrete, *Cem. Concr. Res.* 36 (7) (2006) 1263–1267.
- [7] L. Li, A.G.P. Dabarera, V. Dao, Time-zero and deformational characteristics of high performance concrete with and without superabsorbent polymers at early ages, *Constr. Build. Mater.* 264 (2020), 120262.
- [8] H. Huang, G. Ye, Examining the "time-zero" of autogenous shrinkage in high/ultra-high performance cement pastes, *Cem. Concr. Res.* 97 (2017) 107–114.

- [9] M. Etxeberria, A. Gonzalez-Corominas, The assessment of ceramic and mixed recycled aggregates for high strength and low shrinkage concretes, *Mater. Struct.* 51 (5) (2018) 129.
- [10] H. Zhang, Y.Y. Wang, D.E. Lehman, Y. Geng, Autogenous-shrinkage model for concrete with coarse and fine recycled aggregate, *Cem. Concr. Compos.* 111 (2020), 103600.
- [11] N. Tošić, A. de la Fuente, S. Marinković, Shrinkage of recycled aggregate concrete: experimental database and application of fib Model Code 2010, *Mater. Struct.* 51 (5) (2018) 126.
- [12] V. Revilla-Cuesta, L. Evangelista, J. de Brito, V. Ortega-López, J.M. Manso, Effect of the maturity of recycled aggregates on the mechanical properties and autogenous and drying shrinkage of high-performance concrete, *Constr. Build. Mater.* 299 (2021), 124001.
- [13] M.G. Sohail, R. Kahraman, N. Al Nuaimi, B. Gencturk, W. Alnahhal, Durability characteristics of high and ultra-high performance concretes, *J. Build. Eng.* 33 (2021), 101669.
- [14] J. Xue, B. Briseghella, F. Huang, C. Nuti, H. Tabatabai, B. Chen, Review of ultra-high performance concrete and its application in bridge engineering, *Constr. Build. Mater.* 260 (2020), 119844.
- [15] L. Wu, N. Farzadnia, C. Shi, Z. Zhang, H. Wang, Autogenous shrinkage of high performance concrete: A review, *Constr. Build. Mater.* 149 (2017) 62–75.
- [16] F. Faleschini, M.A. Zanini, C. Pellegrino, S. Pasinato, Sustainable management and supply of natural and recycled aggregates in a medium-size integrated plant, *Waste Manage.* 49 (2016) 146–155.
- [17] J. Sainz-Aja, C. Thomas, I. Carrascal, J.A. Polanco, J. de Brito, Fast fatigue method for self-compacting recycled aggregate concrete characterization, *J. Clean. Prod.* 277 (2020), 123263.
- [18] A.R. Khan, S. Fareed, M.S. Khan, Use of recycled concrete aggregates in structural concrete, *Sustain. Constr. Mater. Technol.* 2 (2019), 149940.
- [19] D. Pedro, J. de Brito, L. Evangelista, Mechanical characterization of high performance concrete prepared with recycled aggregates and silica fume from precast industry, *J. Clean. Prod.* 164 (2017) 939–949.
- [20] R.V. Silva, J. De Brito, R.K. Dhir, The influence of the use of recycled aggregates on the compressive strength of concrete: A review, *Eur. J. Environ. Civ. Eng.* 19 (7) (2015) 825–849.
- [21] R.V. Silva, J. De Brito, R.K. Dhir, Prediction of the shrinkage behavior of recycled aggregate concrete: A review, *Constr. Build. Mater.* 77 (2015) 327–339.
- [22] A. Gonzalez-Corominas, M. Etxeberria, Effects of using recycled concrete aggregates on the shrinkage of high performance concrete, *Constr. Build. Mater.* 115 (2016) 32–41.
- [23] S. Medjigbodo, A.Z. Bendimerad, E. Rozière, A. Loukili, How do recycled concrete aggregates modify the shrinkage and self-healing properties? *Cem. Concr. Compos.* 86 (2018) 72–86.
- [24] Z.H. He, H.B. Hu, I. Casanova, C.F. Liang, S.G. Du, Effect of shrinkage reducing admixture on creep of recycled aggregate concrete, *Constr. Build. Mater.* 254 (2020), 119312.
- [25] R.V. Silva, J. De Brito, R.K. Dhir, Establishing a relationship between modulus of elasticity and compressive strength of recycled aggregate concrete, *J. Clean. Prod.* 112 (2016) 2171–2186.
- [26] Q. Wang, Y. Geng, Y. Wang, H. Zhang, Drying shrinkage model for recycled aggregate concrete accounting for the influence of parent concrete, *Eng. Struct.* 202 (2020), 109888.
- [27] C. Du, A review of magnesium oxide in concrete, *Concr. Int.* 27 (12) (2005) 45–50.
- [28] M. Liska, A. Al-Tabbaa, Ultra-green construction: Reactive MgO masonry products, *Proc. Inst. Civ. Eng.: Waste Res. Manage.* 162 (4) (2009) 185–196.
- [29] F. Jin, A. Al-Tabbaa, Strength and hydration products of reactive MgO-silica pastes, *Cem. Concr. Compos.* 52 (2014) 27–33.
- [30] C. Unluer, A. Al-Tabbaa, Impact of hydrated magnesium carbonate additives on the carbonation of reactive MgO cements, *Cem. Concr. Res.* 54 (2013) 87–97.
- [31] A. Santamaria, F. Faleschini, G. Giacomello, K. Brunelli, J.T. San José, C. Pellegrino, M. Pasetto, Dimensional stability of electric arc furnace slag in civil engineering applications, *J. Clean. Prod.* 205 (2018) 599–609.
- [32] EN 197-1, *Cement – Part 1: Composition, specifications and conformity criteria for common cements* (2011).
- [33] S. Chatterji, Mechanism of expansion of concrete due to the presence of dead-burnt CaO and MgO, *Cem. Concr. Res.* 25 (1) (1995) 51–56.
- [34] L. Mo, M. Deng, M. Tang, Effects of calcination condition on expansion property of MgO-type expansive agent used in cement-based materials, *Cem. Concr. Res.* 40 (3) (2010) 437–446.
- [35] H.M. Tran, A. Scott, Strength and workability of magnesium silicate hydrate binder systems, *Constr. Build. Mater.* 131 (2017) 526–535.
- [36] R. Polat, R. Demirboğa, F. Karagöl, The effect of nano-MgO on the setting time, autogenous shrinkage, microstructure and mechanical properties of high performance cement paste and mortar, *Constr. Build. Mater.* 156 (2017) 208–218.
- [37] H. Ye, Mitigation of drying and carbonation shrinkage of cement paste using Magnesia, *J. Adv. Concr. Technol.* 16 (9) (2018) 476–484.
- [38] P.W. Gao, S.Y. Xu, X. Chen, J. Li, X.L. Lu, Research on autogenous volume deformation of concrete with MgO, *Constr. Build. Mater.* 40 (2013) 998–1001.
- [39] R. Rodríguez-Álvaro, B. González-Fontebo, S. Seara-Paz, K.M.A. Hossain, Internally cured high performance concrete with magnesium based expansive agent using coal bottom ash particles as water reservoirs, *Constr. Build. Mater.* 251 (2020), 118977.
- [40] T. Gonçalves, R.V. Silva, J. de Brito, J.M. Fernández, A.R. Esquinas, Mechanical and durability performance of mortars with fine recycled concrete aggregates and reactive magnesium oxide as partial cement replacement, *Cem. Concr. Compos.* 105 (2020), 103420.
- [41] K. Huang, X. Shi, D. Zollinger, M. Mirsayar, A. Wang, L. Mo, Use of MgO expansion agent to compensate concrete shrinkage in jointed reinforced concrete pavement under high-altitude environmental conditions, *Constr. Build. Mater.* 202 (2019) 528–536.
- [42] R. Polat, R. Demirboğa, W.H. Khushefati, Effects of nano and micro size of CaO and MgO, nano-clay and expanded perlite aggregate on the autogenous shrinkage of mortar, *Constr. Build. Mater.* 81 (2015) 268–275.
- [43] L. Mo, M. Liu, A. Al-Tabbaa, M. Deng, Deformation and mechanical properties of the expansive cements produced by inter-grinding cement clinker and MgOs with various reactivities, *Constr. Build. Mater.* 80 (2015) 1–8.
- [44] R. Wu, S. Dai, S. Jian, J. Huang, H. Tan, B. Li, Utilization of solid waste high-volume calcium coal gangue in autoclaved aerated concrete: Physico-mechanical properties, hydration products and economic costs, *J. Clean. Prod.* 278 (2021), 123416.
- [45] F. Agrela, M. Sánchez De Juan, J. Ayuso, V.L. Gerales, J.R. Jiménez, Limiting properties in the characterisation of mixed recycled aggregates for use in the manufacture of concrete, *Constr. Build. Mater.* 25 (10) (2011) 3950–3955.
- [46] EN 1097-6, *Tests for mechanical and physical properties of aggregates – Part 6: Determination of particle density and water absorption* (2014).
- [47] EN 206, *Concrete – Specification, performance, production and conformity* (2013).
- [48] D. Pedro, J. de Brito, L. Evangelista, Evaluation of high-performance concrete with recycled aggregates: Use of densified silica fume as cement replacement, *Constr. Build. Mater.* 147 (2017) 803–814.
- [49] D. Carro-López, B. González-Fontebo, J. De Brito, F. Martínez-Abella, I. González-Taboada, P. Silva, Study of the rheology of self-compacting concrete with fine recycled concrete aggregates, *Constr. Build. Mater.* 96 (2015) 491–501.
- [50] EN 12350-2, *Testing fresh concrete – Part 2: Slump test* (2020).
- [51] EN 12350-6, *Testing fresh concrete – Part 6: Density* (2020).
- [52] EN 12390-7, *Testing hardened concrete – Part 7: Density of hardened concrete* (2020).
- [53] EN 12504-4, *Testing concrete – Part 4: Determination of ultrasonic pulse velocity* (2006).
- [54] EN 12390-3, *Testing hardened concrete – Part 3: Compressive strength of test specimens* (2020).
- [55] EN 12390-6, *Testing hardened concrete – Part 6: Tensile splitting strength of test specimens* (2010).
- [56] EN 12390-13, *Testing hardened concrete – Part 13: Determination of secant modulus of elasticity in compression* (2014).
- [57] LNEC-E398, *Determination of Drying Shrinkage and Expansion* (in Portuguese), National Laboratory in Civil Engineering (LNEC – Laboratório Nacional de Engenharia Civil), Lisbon, Portugal (1993).
- [58] M. Bravo, J. De Brito, J. Pontes, L. Evangelista, Shrinkage and creep performance of concrete with recycled aggregates from CDW plants, *Mag. Concr. Res.* 69 (19) (2017) 974–995.
- [59] A.M. Soliman, M.L. Nehdi, Effect of drying conditions on autogenous shrinkage in ultra-high performance concrete at early-age, *Mater. Struct.* 44 (5) (2011) 879–899.
- [60] J. Nobre, M. Bravo, J. de Brito, G. Duarte, Durability performance of dry-mix shotcrete produced with coarse recycled concrete aggregates, *J. Buil. Eng.* 29 (2020), 101135.
- [61] D. Pedro, J. de Brito, L. Evangelista, Structural concrete with simultaneous incorporation of fine and coarse recycled concrete aggregates: Mechanical, durability and long-term properties, *Constr. Build. Mater.* 154 (2017) 294–309.
- [62] Y. Yang, B. Chen, Y. Su, Q. Chen, Z. Li, W. Guo, H. Wang, Concrete mix design for completely recycled fine aggregate by modified packing density method, *Materials* 13 (16) (2020) 3535.
- [63] V. Revilla-Cuesta, V. Ortega-López, M. Skaf, J.M. Manso, Effect of fine recycled concrete aggregate on the mechanical behavior of self-compacting concrete, *Constr. Build. Mater.* 263 (2020), 120671.
- [64] K. Ouyang, C. Shi, H. Chu, H. Guo, B. Song, Y. Ding, X. Guan, J. Zhu, H. Zhang, Y. Wang, J. Zheng, An overview on the efficiency of different pretreatment techniques for recycled concrete aggregate, *J. Clean. Prod.* 263 (2020), 121264.
- [65] J. Zhang, G. Ke, Y. Liu, Experimental study on shrinkage reduction of calcium sulphoaluminate cement concrete with addition of pre-wetted lightweight aggregate, *Constr. Build. Mater.* 253 (2020), 119149.
- [66] V. Revilla-Cuesta, M. Skaf, F. Faleschini, J.M. Manso, V. Ortega-López, Self-compacting concrete manufactured with recycled concrete aggregate: An overview, *J. Clean. Prod.* 262 (2020), 121362.
- [67] J. Nobre, H. Ahmed, M. Bravo, L. Evangelista, J. de Brito, Magnesia (MgO) production and characterization, and its influence on the performance of cementitious materials: A review, *Materials* 13 (21) (2020) 4752.
- [68] R. Kurda, J. de Brito, J.D. Silvestre, Water absorption and electrical resistivity of concrete with recycled concrete aggregates and fly ash, *Cem. Concr. Compos.* 95 (2019) 169–182.
- [69] V. Corinaldesi, Mechanical and elastic behaviour of concretes made of recycled-concrete coarse aggregates, *Constr. Build. Mater.* 24 (9) (2010) 1616–1620.
- [70] Z. Prošek, V. Nežerka, R. Hlůžek, J. Trejbal, P. Tesárek, G. Karra'a, Role of lime, fly ash, and slag in cement pastes containing recycled concrete fines, *Constr. Build. Mater.* 201 (2019) 702–714.
- [71] M. Mavroulidou, T. Morrison, C. Unsworth, M.J. Gunn, Properties of concrete made of multicomponent mixes of low-energy demanding binders, *Constr. Build. Mater.* 101 (2015) 1122–1141.
- [72] V.M. Malhotra, *Testing Hardened Concrete: Nondestructive Methods*, American Concrete Institute Monograph, Iowa State University Press, Ames IA, Iowa, USA, 1976.